NTNU

Norwegian University of
Science and Technology

Area Based Frequency Control in the Nordic Power System

Tarje Moe Sandvik

Master of Science in Cybernetics and Robotics
Submission date: June 2016
Supervisor: Lars Imsland, ITK
Co-supervisor: Eivind Lindeberg, Statnett SF

Norwegian University of Science and Technology
Department of Engineering Cybernetics

Abstract

Automatic frequency restoration reserves (FRR-A) are used for restoring the electric frequency when disturbances in the power network occur. Currently the whole Nordic power system's secondary frequency control is based on one PI-controller for the whole synchronous area. This thesis explores the possibilities for an alternate control structure for FRR-A in the Nordic region by the use of several autonomous controllers.

A linear model of a hydro power generating unit is used to model control areas with tie-line connections to neighbouring areas. The tie-line power exchange is modelled using DC load flow. MATLAB and Simulink are used to simulate a power system resembling the Nordic synchronous region.

The control strategy chosen is based on a traditional AGC integral controller in each area to minimize the frequency and tie-line flow error. The output from the local secondary controllers is sent to a control centre where FRR-A bids from generating companies are activated automatically. A MILP optimization problem chooses the cheapest FRR-A bids, constrained by tie-line capacities. The optimal setpoints and desired tie-line flows are fed back to each control area.

The results show that the control structure succeeds in restoring the frequency as well as minimizing costs and handling capacity constraints. The optimization time is within the speed requirements for eleven control areas and large bid lists.

Sammendrag

(Norwegian Translation of the Abstract)
Formålet med automatiske sekundærreserver (FRR-A) er å bringe frekvensen tilbake til 50 Hz når ubalanser i kraftsystemet oppstår. I dag styres dette av én PI-regulator for hele Norden. Med dette som bakgrunn undersøker oppgaven muligheter for en alternativ kontrollstruktur for FRR-A, med én regulator i hvert kontrollområde.

En linær model av kontrollområder er modullert og simulert i MATLAB og Simulink for å etterligne det nordiske kraftnettet. Kraftflyt mellom områder er modellert ved hjelp av DC load flow approksimasjon.

Løsningen anvender lokale AGCer som minimerer flyt og frekvensavvik. Utgangen fra de lokale sekundærregulatorene blir sent til et kontrollsenter, hvor FRR-A-bud fra produksjonsselskaper blir aktivert automatisk. Et MILP optimaliseringsproblem velger de billigste budene og tar samtidig hensyn til overføringskapasitet. Referanseverdier for flyt og produksjon blir deretter sent tilbake til hvert underområde.

Resultatene viser at metoden bringer frekvensen tilbake til 50 Hz, samtidig som overføringskapasiteter er overholdt. Kjøretiden til allokeringsalgoritmen er innenfor tidskravet, simulert med elleve kontrollområder og mange tilgjengelige bud.

Preface

This thesis was written in collaboration with Statnett SF as a part of the Master of Technology program in Engineering Cybernetics at NTNU.

It has been motivating to work on an actual problem in the Nordic power system and I have learned a lot since I started the research in January. As well as the technical aspect of the thesis, I found the assignment itself highly motivating, as balancing power demand and supply is essential to introduce more renewable energy sources to the power system in the future.

I would like to thank my supervisor, Lars Imsland at the Department of Engineering Cybernetics for useful advice and guidance and my co-supervisor at Statnett SF, Eivind Lindeberg, for (patiently) helping me understand concepts in the Nordic power system and for an interesting and challenging assignment. I would also like to thank Kjetil Uhlen at the Department of Electrical Power Engineering for helping me with questions regarding power systems.

Thank you to my fellow M.Sc. students from room G232 for a light-hearted work environment, technical and moral support and long lunch breaks. Finally, I want to thank Studentersamfundet i Trondhjem and my friends from the stage and lighting crew, Regi, for teaching me all those things that a university cannot teach you.

Tarje Moe Sandvik
Trondheim, June 2016

Table of Contents

List of Tables

List of Figures

Abbreviations

AC	Alternate current
AGC	Area generation control
ATC	Available transfer capacity
DC	Direct current
DCLF	Direct current load flow
DISCO	Distribution company
FCR	Frequency containment reserves
FCR-D	Frequency containment reserves for disturbances
FCR-N	Frequency containment reserves for normal operating band
FRR-A	Automatic frequency restoration reserves
FRR-M	Manual frequency restoration reserves
GENCO	Generation company
ISO	Independent System Operator
KKT	Karush–Kuhn–Tucker
LFC	Load frequency control
LP	Linear rogramming
MILP	Mixed integer linear programming
MPC	Model predictive control
PI	Proportional, integral
RES	Renewable energy sources
RKOM	Market for FRR-M
TSO	Transmission system operator
UFLS	Under-frequency load shedding

Chapter 1

Introduction

1.1 Motivation

Power systems around the world are continuously being developed to meet new demands. Open power markets, distributed generation and increasing amount of intermittent renewable energy sources makes the power system harder to regulate. Power is a commodity and the power generated has to equal the power consumed at all times. This is mostly regulated by the power market, where generation and distribution companies trade power based on the current and predicted demand. The open power market settles at a production level for every hour of the day. Every change in load interior the operating hour will cause a difference in generation and consumption, thus causing the power frequency to change accordingly. The frequency is therefore a measure of the imbalance between generation and consumption.

The Nordic power system is a synchronous area with a common frequency. Disturbances affect the whole area, and the countries are dependent on each other to maintain satisfactory operation. As the Norwegian *transmission system operator* (TSO), Statnett is responsible for secure and effective operation of the power system. This includes keeping the frequency within reasonable limits at all times along with coordinating trade with other countries and determine captivities in the power network. The nominal frequency in the Nordic power system is 50 Hz. Data from (Statnett SF, 2014), shown in Figure 1.1, shows an increase in minutes outside of the accepted frequency since 2007. This is due to factors such as increased production from renewable energy sources like wind power (Ersdal et al., 2015b) and a tighter connection to the European power system. These trends are predicted to continue, with 1000 MW wind power commissioned in central Norway (Statkraft, 2016) and a new cable connecting the Norwegian and German power grid (Statnett SF, 2016). The power system therefore needs to handle greater disturbances in both production and consumption in the future.

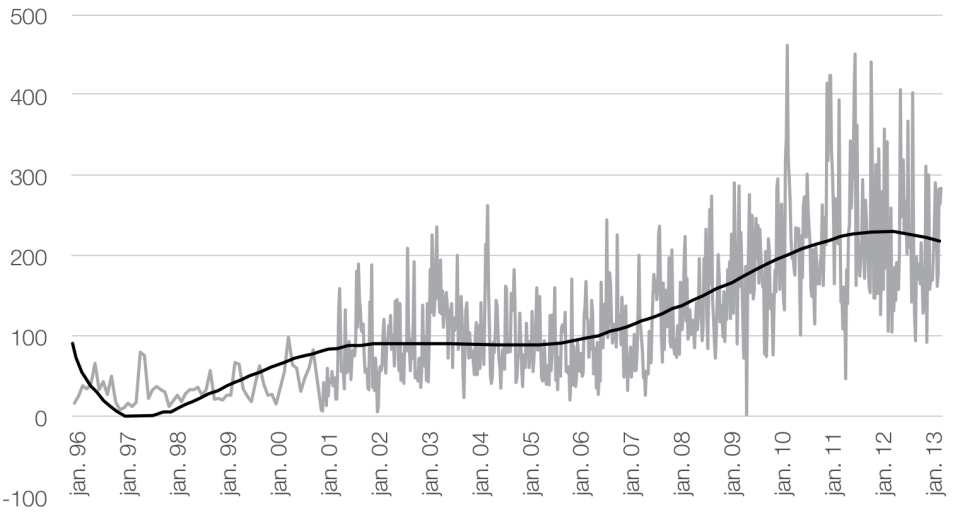

Figure 1.1: Minutes of frequency error outside limits. (Statnett SF, 2014)

Automatic secondary reserves (FRR-A) have recently shown a positive effect on the frequency quality (Statnett SF, 2014). An FRR-A market for the Nordic countries is under development, where flexibility can be bought within the operating hour. This will open up for competition among generation companies (GENCOs) and allow secondary power reserves to be activated where it is cheapest, hence reducing costs for maintaining the nominal frequency. For this thesis, it is assumed that such a market exists so that secondary reserves are available in the form of bids from generation companies and can be activated automatically by the TSO. With a better system for FRR-A and an established market for power flexibility, Norwegian hydro power can help balance intermittent renewable energy sources, not only in Norway, but in the Nordic synchronous area and Europe (Statnett SF, 2016).

1.2 Literature Review

Frequency control is an important control problem in electronic power system design and is becoming more significant today due to the increasing size and complexity of power systems, changing structure, emerging new distributed and renewable energy sources. (Bevrani, 2014) gives a thorough explanation of the frequency control hierarchy, presents simple models for power systems and analyses different control strategies. (Shayeghi et al., 2009) gives an historical overview of control strategies for load frequency control.

(Ersdal et al., 2015a) uses centralized model predictive control (CMPC) for load-frequency control and compares it to a traditional AGC scheme with PI-controllers. It is simulated using a complex model of the Nordic power system from SINTEF, and a linear model described in (Bevrani, 2014) for the model based prediction. Results show that applying

MPC to AGC can lead to both better control performance and a reduction in use of reserves. (Venkat et al., 2008) and (Mohamed et al., 2011) are examples of distributed or decentralized model prediction control (DMPC) applied to LFC, where each control area has its own MPC. This reduces the model for each area and makes the optimization problem smaller, which is beneficial considering large power systems, such as in continental Europe or North America. (Beaufays et al., 1994) approaches the problems using trained neural networks. Different method for decentralized and distributed MPC is reviewed in (Scattolini, 2009).

Predicting power flows in an electrical grid is challenging due to the physics of the power systems: Kirchoff's laws are global and in order to calculate the tie-line flows in an electric grid, all states in the network must be known. Approximations can be made, such as the *Direct Current Load Flow* method. A lot of literature exists on this topic, like (Schavemaker and Van Der Sluis, 2008). Decentralized methods for solving DC load flow is presented with promising results in (Bakirtzis and Biskas, 2002; Conejo and Aguado, 1998; Bakirtzis and Biskas, 2003).

Good sources for basic control theory are (Balchen et al., 2003; Åström and Hägglund, 2006) and (Nocedal and Wright, 2006) is a good source for numerical optimization.

1.3 Objective of Thesis

Currently, the secondary reserves are controlled by one PI-controller for the whole Nordic power system. The cheapest bids are activated, based on the total demand from the PI-controller. This is however not a fully automated service at the moment and considerations regarding flow capacities and bottlenecks have to be handled manually. The goal of this thesis is to explore the possibilities for a new control structure, with separate autonomous controllers for each control area and an automatic strategy for choosing which FRR-A bids to activate. Although this is a conceptual study, the thesis strives to propose a solution that is practically possible to implement in the Nordic power system. A secondary objective is therefore to keep the control strategy complexity low for easy implementation and fast enough to work in a real-time environment. The control strategy should work on any number of control areas, and new control areas should be easy to add to the system. The implementation in Simulink should therefore be module based and easy to expand.

1.4 Structure of Thesis

Chapter 2 explains the basic theory used in the model of the power system, frequency control and optimization. Chapter 3 presents the modelling of the power system and the primary and secondary control loops, and a centralized FRR-A allocation algorithm is presented in Chapter 4. Simulation results are presented in Chapter 5 and discussed in Chapter 6. A final conclusion is given in Chapter 7 along with suggestions for future work.

Chapter 2

Background Theory

This chapter provides some of the basic theory and background information that is needed to comprehend the material presented throughout the thesis. The concept of frequency control is explained and an overview of the Nordic power system and market for power reserves is given. Secondly, optimization theory used in the thesis is explained.

2.1 Power System Frequency Control

Frequency deviation is a direct result of the imbalance between the electrical load and the power supplied by the connected generators. Off-normal frequency deviation can cause damage to equipment, overloading of transmission lines and trigger protection devices. If the frequency falls too much, it can cause generators to trip, creating a domino effect and a total collapse of the power system.

When disturbances happen, the frequency changes. Disturbances can be both in load and production: The actual load will differ somewhat from the predicted load and will vary every time a light switch is flipped on or off. Production may also vary due to generators failing to produce as scheduled, turbines tripping, failures on transmission lines etc. The power system must be robust to these disturbances and the strategy today is a hierarchical approach, depending on the magnitude and duration of a disturbance. A simplified illustration of a power generating unit is shown in Figure 2.1 and the time perspective of the three typical frequency control loops is illustrated in Figure 2.2.

In power systems analysis, the *per-unit* system is used to express quantities defined by a base unit quantity. This is an advantageous representation for generators of different sizes. All states of power in this thesis, will therefore be in *per-unit* representation, and then multiplied with the base unit quantity in the results.

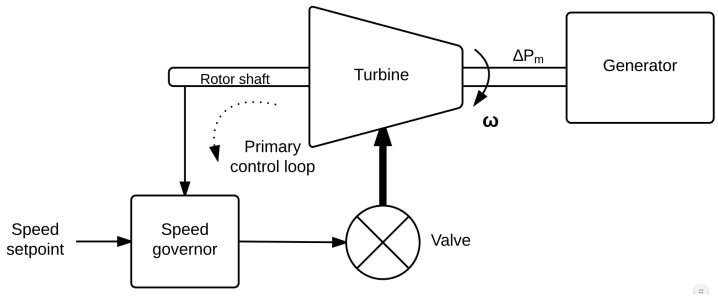

Figure 2.1: Generating unit with primary control. ω is the rotation speed of the generator.

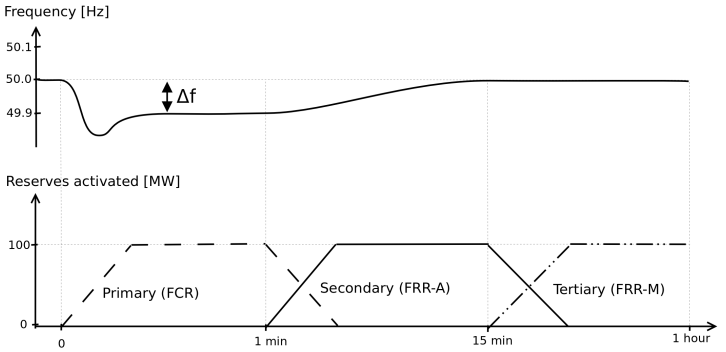

Figure 2.2: Control stages following a 100 MW load disturbance.

2.1.1 Primary Control

Turbine generators have stored kinetic energy due to their large rotating masses. All the kinetic energy stored in a power system in such rotating masses is a part of the grid inertia. When system load increases, grid inertia is initially used to supply the load. This, however, leads to a decrease in the stored kinetic energy of the turbine generators. Since the mechanical power of these turbines correlates with the delivered electrical power, the turbine generators have a decrease in angular velocity, which is directly proportional to a decrease in frequency in synchronous generators (Glover et al., 2011). As shown in Figure 2.1, the flow into the turbine is regulated by a speed governor, which has a feedback from the rotation speed of the rotor shaft. The rotation speed error is fed into a fast controller (eg. PID-controller), that adjusts the flow into the turbine. This maintains the rotation speed of the generator and is referred to as the *primary control loop*. The response time of the primary reserves is from a few seconds to several minutes. The rotation speed setpoint can be adjusted, in order to make the generator run faster or slower.

Droop

An important characteristic of the primary loop is the droop, ρ. As shown in Eq. (2.1), the droop is a measure of the steady-state frequency deviation in percent, when the primary

control is at maximum.

$$\frac{\Delta f_{stationary}}{f_N} = \rho \Delta P_m \tag{2.1}$$

$\Delta f_{stationary}$ is the stationary frequency deviation in Hz, $f_N = 50Hz$ the nominal frequency, ρ the droop in percent and ΔP_m the generator mechanical power change in *per unit*. The lower the percentage, the more aggressive is the primary controller response to a frequency change, hence reducing the frequency stationary error.

2.1.2 Secondary Control

When a disturbance occurs, the frequency starts to deviate from the nominal frequency and the generator's angular velocity is affected. The primary control loop restores the generator's rotation speed, and the frequency stabilizes. This creates a stationary error from the nominal frequency and motivates the need for an outer control loop, with a feedback from the electrical frequency. This secondary control loop restores the frequency back to the nominal value, by adjusting the setpoint of the primary loop. In order to restore the frequency after a load increase, the speed of the generators will have to run at a faster speed for some time. As the two controllers are connected in series, the time constant of the outer loop should to be slower than the inner loop (Åström and Hägglund, 2006). As seen from the time perspective in Figure 2.2, the secondary control operates from 15 seconds to 15 minutes after a disturbance. Secondary control is commonly referred to as *Load Frequency Control* (LFC), *Area Generation Control* (AGC) or *Automatic Frequency Restoration Reserves* (FRR-A). The secondary loop is often automatic and its main task is to restore the frequency and relieve the primary control, so that it is ready to handle new disturbances.

AGC can be used to both regulate the frequency and to maintain the power exchange with neighbouring areas to a scheduled value. Based on the two objectives, the frequency and the tie-line power exchanges are weighted together by a linear combination to form a single variable called *Area Control Error* (ACE) as shown in Eq. (2.2), which is used as the control signal in the secondary loop. The secondary control is typically a PI-controller.

$$ACE = \beta \Delta f + (\Delta P_{tie} - \Delta P_{tie,d}) \tag{2.2}$$

Δf is the frequency deviation in *hertz*, β is the secondary gain, which equals how much electrical power (in *per-unit*) 1Hz frequency deviation represents. $\Delta P_{tie,d}$ is the desired tie-line flow out of the area and ΔP_{tie} is the measured flow.

As a control area normally consists of multiple generating units, the secondary contribution from each generating unit is defined by participation factors, α, which together add up to 1.

2.1.3 Tertiary Control

For serious load-generation imbalances, the secondary control may be unable to restore the frequency and it is necessary to activate even more production to restore the frequency. Tertiary reserves may also be activated to free the secondary control, so that it can handle new disturbances. This is often done manually and is referred to as *Manual Frequency Restoration Reserves* (FRR-M). As seen from the time overview in Figure 2.2, this is a slow service with an activation time over 15 minutes. Further emergency control actions can be taken if the frequency is still outside the limits to prevent damages in the system, like under-frequency load shedding (UFLS) where load is disconnected to restore stability.

2.2 The Nordic Power System

Table 2.1 shows the types of production in Norway, Sweden, Denmark and Finland on a weekday afternoon in May. Hydro power is the most flexible type of production and contributes the most to balancing services. Denmark has mostly wind power, which is an intermittent energy source, naturally dependent on the current wind and with no reserves. If there is no wind, the wind generators will not produce anything, and Denmark is therefore relying on flexibility from Norway and Sweden in order to have power at all times. When there is high wind production Denmark, the hydro plants can be down-regulated, in order to take advantage of the available wind energy.

	NO [MW]	**SE [MW]**	**DK [MW]**	**FI [MW]**	**Total [MW]**
Hydro	16 960	8 799	-	2 398	28 157
Nuclear	-	5 895	-	1 799	7 694
Heat	98	353	1 514	2 398	4 363
Wind	65	1 236	1 194	61	2 556
Other	-	451	-	26	477
Total	**17 123**	**16 735**	**2 708**	**6 587**	**43 153**

Table 2.1: Power production in the Nordic power system at 14:37 on May 24, 2016 (www.statnett.no, 2016).

A map of the Nord Pool Spot pricing areas is shown in Figure 2.3. The Nordic synchronous area consists of Norway (NO1, NO2, NO3, NO4, NO5), Sweden (SE1, SE2, SE3, SE4), Finland (FI) and parts of Denmark (DK2). The frequencies will be similar in theses areas. DK1 is included in the Nord Pool Spot system, but is not a part of the synchronous area. As a disturbances in one area affects the whole synchronous system, the countries TSO's must cooperate in order to balance the system.

2.2.1 Frequency Control in the Nordic Synchronous Area

The Nord Pool Spot market settles at a point where the predicted demand is met for the next operation hour. Every disturbance or deviation from predicted load is handled by the primary *Frequency Containment Reserves* (FCR), secondary *Automatic Frequency Restora-*

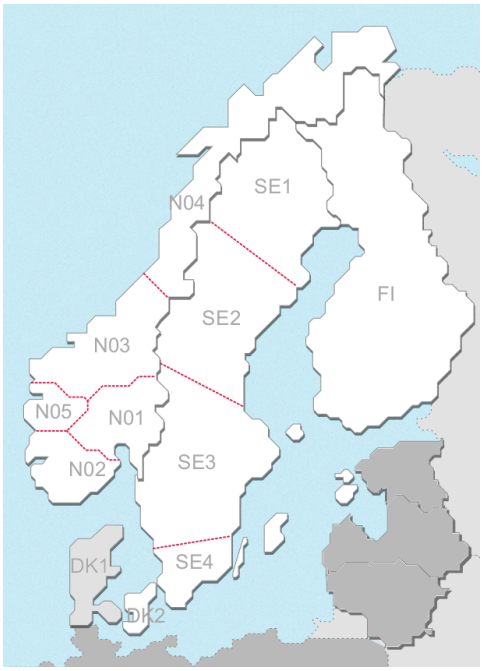

Figure 2.3: The Nordic power system with Nord Pool Spot areas

tion Reserves (FRR-A) and tertiary *Manual Frequency Restoration Reserves* (FRR-M).

Currently, FCR can be bought on a weekly and daily market, while FRR-A is only reserved on a weekly basis. As claimed in (Eivind Lindeberg, 2014), the secondary reserves need to be of a certain quantity, in order to have a noticeable effect. While a total of 100MW FRR-A makes a small difference, 350MW strongly reduces minutes of frequency error outside acceptable limits. During test periods, FRR-A has been proven expensive for Statnett and has only been available for hours of the day when the balancing task statistically tends to be the most challenging. A report from Landssentralen at Statnett (Statnett SF, 2015) shows that FCR costs about 100 MNOK yearly, while the use of FRR-A has varied between 12 MNOK and 62 MNOK yearly since it was implemented in 2012.

Generation companies have to meet certain demands from Statnett, and some requirements from (Statnett SF, 2012a,c) are outlined:

- All generators over 10MW should have a primary controller with adjustable droop. The droop should be between 4% and 12%.
- Generating units contributing to FRR-A should have a maximum activation time of 120 seconds (illustrated in Figure 2.4).
- FRR-A setpoints can be set externally by Statnett.

- FRR-A bids must be UP or DOWN and should be dividable by 5MW.
- The provider may deliver both FRR and FCR from the same station/generator at the same time.

(Statnett SF, 2012b) describes the interface between Statnett's load frequency control and the providers AGC.

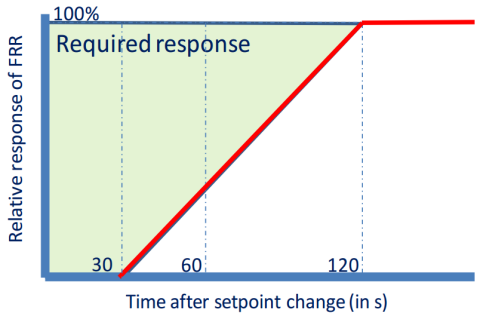

Figure 2.4: FRR-A activation requirement (Statnett SF, 2012c)

2.3 Direct Current Load Flow

Power flow computations are essential in power system analysis. In some situations, the use of full AC flow computations may be difficult or unnecessarily complicated. Large power network, or situations where knowledge about voltage control and reactive resources are limited, provokes the need for an approximation of the power flow. A good alternative is to use *Direct Current Load Flow* (DCLF). It is a linear method and is increasingly used in the power system community for power market and congestion management analyses (Uhlen, 2015). (McCalley, 2012) describes the DC load flow method and is briefly outlined in the following. Consider a power system of n nodes and m branches (tie-lines). $j \in [1, n]$ and $k \in [1, n]$ represents nodes and $i \in [1, m]$ represents branches. From (McCalley, 2012), the power flow equations from node k are given as:

$$\begin{aligned} P_k &= \sum_{j=1}^{N} |V_k||Vj| \Big[G_{kj} \cos(\theta_k - \theta_j) + B_{kj} \sin(\theta_k - \theta_j) \Big] \\ Q_k &= \sum_{j=1}^{N} |V_k||Vj| \Big[G_{kj} \sin(\theta_k - \theta_j) - B_{kj} \cos(\theta_k - \theta_j) \Big] \end{aligned} \tag{2.3}$$

where P_k and Q_k is the active and reactive power flow from node k. V is the nodal voltages, G the conductance, B the susceptance and j is the set of connected nodes.

For a high voltage electric transmission system, three practical assumptions can be made:

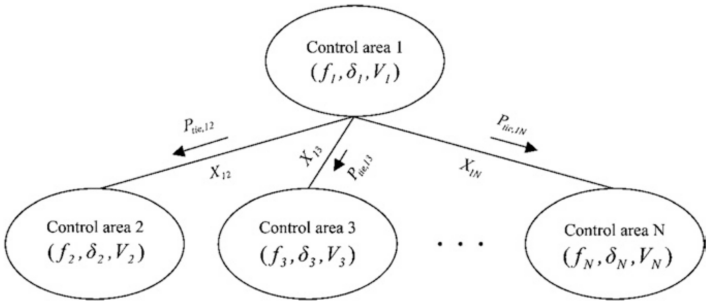

Figure 2.5: Example of interconnected power system with N nodes. Line reactances are shown as X.

1. The voltage profile in the grid is uniform such that all voltages are close to nominal. Therefore, in per-unit, all nodal voltages are assumed to be $U_k = 1.0$.
2. The reactances of tie-lines are significantly greater than the resistance ($X_i \gg R_i$), and all resistances are neglected.
3. For most typical operating conditions, the difference in angles of the voltage phasors at two nodes ($\theta_k - \theta_j$) is less than 10-15 degrees. A good approximation is therefore $\sin(\theta_k - \theta_j) = \theta_k - \theta_j$ and $\cos(\theta_k - \theta_j) = 1$

Only the active power flow is of interest in the approximation and with the assumptions the active power flow in Eq. (2.3) simplifies to:

$$P_k = \sum_{\substack{j=1 \\ j \neq k}}^{N} B_{kj}(\theta_k - \theta_j) \tag{2.4}$$

Real power flow is now determined only by the susceptance of the tie-line, B_i, and the difference in voltage phasor angles, ($\delta_i = \theta_k - \theta_j$), between the nodes.

2.3.1 Matrix Form

The real power flow in matrix form is given in Eq. (2.5) for a power network with n nodes and m branches.

$$\vec{P} = \boldsymbol{B'}\vec{\theta} \tag{2.5}$$

where $\vec{P} \in \mathbb{R}^n$ is the vector of nodal injections, $\vec{\theta} \in \mathbb{R}^n$ is the vector of nodal phase angles and $\boldsymbol{B'} \in \mathbb{R}^{n \times m}$ is the *B-prime matrix* which is further described. It has the negative susceptance of branch i at $\boldsymbol{B'}(j,k)$ and $\boldsymbol{B'}(k,j)$ and the sum of all susceptances excluding B_i on the diagonal $\boldsymbol{B'}(i,i)$. As the equation is based on phasor angle differences, one node is set as the reference with $\theta = 0$.

The flow of the system, given the power injections, $\vec{P}$, is given in Eq. (2.6).

$$\vec{P_{flow}} = \boldsymbol{DA\theta} \tag{2.6}$$

where $\boldsymbol{D} \in \mathbb{R}^{m \times m}$ has non-diagonal elements of zero and $\boldsymbol{D}(i,i)$ contains the negative susceptance of branch i. $\boldsymbol{A} \in \mathbb{R}^{m \times n}$ is the adjacency matrix, or connection matrix. Each row represents one branch and the beginning node (j) and end node (k) are represented respectively with $\boldsymbol{A}(i,j) = 1$ and $\boldsymbol{A}(i,k) = -1$. The rest of the elements are zero.

2.3.2 Laplace Transfer

Linearizing Eq. (2.4) around an equilibrium point (θ_j^0, θ_k^0) gives:

$$\Delta P_{tie,jk} = B_{jk}(\theta_j - \theta_k) \tag{2.7}$$

Based on the relationship between power angle and frequency, Eq. (2.7) can be rewritten as:

$$\Delta P_{tie,jk} = 2\pi B_{jk} \int (\Delta f_j - \Delta f_k) \tag{2.8}$$

which is given in Laplace transform

$$\Delta P_{tie,jk} = \frac{2\pi}{s} B_{jk}(\Delta f_j - \Delta f_k) \tag{2.9}$$

The total tie-line flow out of area j is given by

$$\Delta P_{tie,j} = \sum_k \Delta P_{tie,jk} \tag{2.10}$$

where k is the set of all areas connected to area j.

2.4 Optimization

The basic theory behind the optimization used in the thesis is briefly explained and literature sources are given in this section.

2.4.1 Linear Programming

Linear programming and the simplex method continue to hold sway as the most widely used of all optimization tools (Nocedal and Wright, 2006). Even though the nature of a system is non-linear, linear programming is appealing because of the advanced state of the software, guaranteed convergence to a global minimum, and the fact that uncertainty in the model makes a linear model more appropriate than an overly complex nonlinear model. Linear programs have a linear objective function and linear constraints, which may include both equalities and inequalities, and the feasible set is a convex polytope, as shown in Figure 2.6. The linear program is infeasible if the feasible set is empty. Linear programs are usually stated in the following standard form:

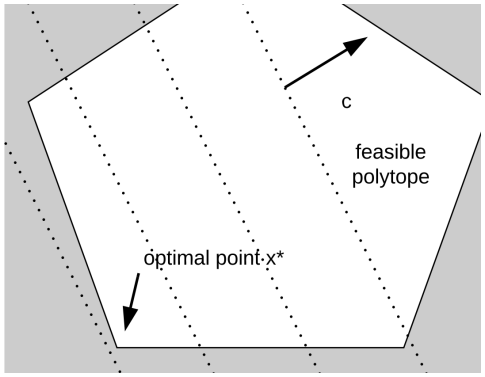

Figure 2.6: A linear program in two dimensions with optimal solution at x^*.

$$\begin{array}{lrcl} \min\limits_{x} & c^T x & & \\ \text{s.t.} & Ax & = & b \\ & x & \geq & 0 \end{array} \tag{2.11}$$

where $x \in \mathbb{R}^n$ is the state vector, $c \in \mathbb{R}^n$ is a constant cost matrix which penalizes the states and $b \in \mathbb{R}^m$ and $A \in \mathbb{R}^{m \times n}$ are constant and defines the constraints. Any linear programs can be transformed into this form. Inequality constraints can be represented in the standard form by introducing slack variables.

2.4.2 Mixed Integer Linear Programming

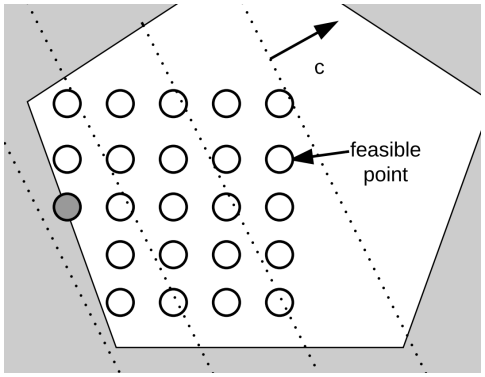

Figure 2.7: A mixed integer linear program in two dimensions with optimal solution (gray circle).

Mixed-integer linear programming expands the linear programming problem with the additional constraint that some or all of the variables in the optimal solution must be integers. The feasible set is still a polytope, but with some values restricted to integers. An illustration is shown in Figure 2.7. The feasible region consists of a set of disconnected integer

points and gradient-based algorithms cannot be directly applied. Also, first order optimality cannot be proven with conditions similar to the KKT conditions. Integer programming is originally NP-hard, but methods exists that can solve the problem quickly under certain assumptions.

Chapter 3 in (Pochet and Wolsey, 2006) explains mixed integer linear programming thoroughly. The two basic algorithms for solving MILPS are branch-and-bound and branch-and-cut. Branch-and-bound is a divide and conquer approach: break problem into subproblems (sequence of LPs) that are easier to solve (Knudsen, 2015) and is thoroughly explained in (Bénichou et al., 1971). (Bixby et al., 2000) explains the basics for the branch and cut method and is briefly outlined here: The algorithm begins by solving the linear-programming relaxation, obtained by simply deleting the integer restrictions. If the solution $x*$ of this LP satisfies all the integer restrictions, the solution is found; otherwise, some integer restriction is violated. Picking an integral variable x_j that is currently fractional with value x_j*, we branch, creating two separate *child problems* from the single *parent problem*, one of which has the added restriction $x_j \leq \lfloor x_j* \rfloor$ and the other of which has the added restriction $x_j \geq \lceil x_j* \rceil$. At any point, if a cutting plane is identified that cuts off the solution to the current LP, that constraint is added to the LP. The procedure is repeated.

Chapter 3

Power System Model

The Nordic synchronous power system is modelled as eleven separate control areas and the Pool Spot Pricing areas shown in Figure 2.3 are used to define each area. The model for an area should be module-based, so that it is easy to add new areas or change its parameters. Each area is therefore modelled identically, but with the option of changing the model parameters from the outside. As the thesis' primary focus is on the control strategy, the complexity of the power system model is low, but with enough dynamic properties to resemble the primary control response. The model chosen is based on a well known and linear model presented in (Bevrani, 2014). The model is somewhat extended and parameters are adjusted to obtain the characteristics of the Nordic power system. This chapter describes the control area model, including primary and secondary control and the tie-lines between areas.

3.1 Control Area Model

The control area is modelled as one hydro generating unit with primary and secondary control and is shown in Figure 3.1. The Simulink implementation is shown in Appendix B. Since the control area only has one generating unit, there is no need or participation factors, as one unit represents all production in one area. All states, except Δf are in *pu* (per-unit), which means they have to be multiplied with the power base value, P_{base} in order to get values in megawatts. All states are deviations from hourly scheduled production and flow. Disturbances are modelled as a load change, ΔP_L. Note that the load-change models a generation-production mismatch, and can in theory also represent a production disturbance. With no disturbances, all states will be zero, which corresponds to the hourly scheduled power production, tie-line flow and a frequency of $f = f_N = 50$Hz.

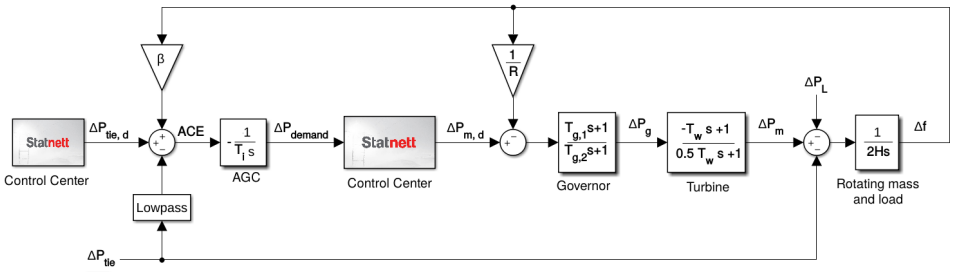

Figure 3.1: Control area model with primary and secondary control. The *Statnett* blocks show the interaction with the Control Center (introduced in the next Chapter).

3.1.1 Primary Loop

The primary loop is described in Section 2.1. The governor, turbine and the rotating mass and load of the generator are modelled with transfer functions given in Figure 3.1. The droop is proportional to $1/R$ in the model, which is the feedback gain in the primary loop, and the relation is shown in (3.1).

$$R = f_N \cdot \rho = 50\rho \tag{3.1}$$

Due to requirements from Statnett mentioned in Section 2.2.1, droop between 4% and 12% is chosen as the control area droops in the simulations. A droop of 8% corresponds to $R = 4$ according to Eq. (3.1). This means that the primary control is at maximum when the frequency deviates with 8% or $\Delta f = \rho \cdot f_N = 0.08 \cdot 50Hz = 4Hz$. Parameters for all 11 control areas are shown in Table 3.1. The time constant for the governor, turbine

Area	T_w **[s]**	H **[s]**	$T_{g,1}$ **[s]**	$T_{g,2}$ **[s]**	R **[Hz/pu]**	β **[pu/Hz]**	T_i **[s]**
NO1	1.5	3.5	5	30	4.00	0.26	200
NO2	1.5	3.5	5	30	4.17	0.25	200
NO3	1.5	3.5	5	30	4.00	0.25	200
NO4	1.5	3.5	5	30	2.86	0.34	200
NO5	1.5	3.5	5	30	3.33	0.26	200
SE1	1.5	3.5	5	30	3.85	0.27	200
SE2	1.5	3.5	5	30	4.00	0.26	200
SE3	1.5	3.5	5	30	4.35	0.24	200
SE4	1.5	3.5	5	30	4.55	0.23	200
FI	1.5	3.5	5	30	4.55	0.25	200
DK2	1.5	3.5	5	30	5.56	0.19	200

Table 3.1: Parameters and control gains for the power system model.

and generator (rotating mass and load) are set equal for all areas. Regulation strengths are,

however, varied with the lowest strength in DK2 ($R_{DK2} = 5.56$ Hz/pu, corresponding to $\rho_{DK2} = 11.12\%$) and the highest strength in NO4 ($R_{NO4} = 2.86$ Hz/pu, corresponding to $\rho_{NO4} = 5.72\%$). The areas are assigned parameters randomly, to test that the control strategy works for an interconnected region with different area characteristics. The average of model parameters, droops and control gains are set to resemble the characteristics of the Nordic Power system, but are not an accurate representation for the specific areas. All areas has the same power base value, $P_{base,area} = 2500MVA$, and the total base for the whole system is therefore $P_{base,system} = 2500MVA \cdot 11 = 27500MVA$. The total droop for the system is simply the average of the area droops $\rho_{system} = \sum_{i=1}^{11} \frac{\rho_i}{11} = 0.08 = 8\%$.

3.1.2 Secondary Loop

The secondary control loop is a crucial part of the overall control strategy, as it works as a demand estimator for each area, which the Control Center bases its decisions on. Before it is used as a demand estimator, it will therefore be tested in the simulation, where the output is passed directly to the primary loop as a setpoint. The ACE signal will in these tests have a desired tie-line $\Delta P_{tie_d} = 0$, which will drive all production to where the disturbance happened. This control strategy is shown in Figure 3.2 and will be referred to as *Standard AGC*.

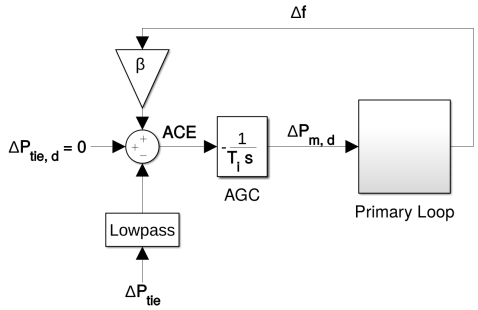

Figure 3.2: Block diagram of *Standard AGC* concept. ΔP_{tie} is the measured tie-line flow. $\Delta P_{tie,d}$ is the desired tie-line flow, set by the FRR-A control center and the *Area Control Error* (ACE) is given in (2.2).

The ACE signal is used as input to a PI-controller. The proportional gain is sensitive to the oscillations in the power frequency and is therefore set to zero. The controller in the implementation is therefore a simple integral controller shown in Eq. (3.2). The controller will force the local frequency error to zero, as well as achieve the desired tie-line flow. A deviation in tie-line flow will cause the integral controller to change the primary control setpoint, $\Delta P_{m,d}$, and the power produced, ΔP_m, will adjust accordingly.

$$\Delta P_m = -\frac{1}{T_i s}(ACE) \tag{3.2}$$

3.2 Tie-lines

The control areas are connected by tie-lines and the DC load flow approximation is used to model the flow. From Eq. 2.10, the power flow out of an area is the integral of the frequency difference to connected areas multiplied by a constant. To represent a variety of damping sources in the system, a damping term is added with coefficient $D = 0.05$ to the power flow between areas, so the equation now becomes:

$$\Delta P_{tie,jk} = \frac{2\pi}{s} B_{jk}(\Delta f_j - \Delta f_k) + DB_{jk}(\Delta f_j - \Delta f_k) \tag{3.3}$$

The tie-line flows are modelled in a separate Simulink block with the local frequencies as input and the tie-line flows as output. Table 3.2 shows an overview of the 16 modelled tie-lines, connecting the 11 control areas. The tie-line admittances are set to achieve power flow oscillations of about 0.5Hz, which is normal in the Nordic network (Chaudhuri et al., 2010). The value for each specific tie-line is selected randomly and is not an attempt to model that specific tie-line. Note that the admittance only consists of the imaginary part since the conductance is set to zero (as described in Section 2.3).

Tie-line number	From - To	Admittance
1	NO1-NO2	3.00
2	NO1-NO3	3.10
3	NO1-NO5	2.90
4	NO1-SE3	3.15
5	NO2-NO5	2.98
6	NO3-NO5	2.95
7	NO3-NO4	3.16
8	NO3-NO2	2.97
9	NO4-SE1	3.01
10	NO4-NO2	2.87
11	NO4-FI	3.22
12	SE1-SE2	3.14
13	SE1-FI	2.89
14	SE2-SE3	2.95
15	SE3-SE4	2.85
16	SE4-DK2	3.01

Table 3.2: Tie-line connections between control areas

Chapter 4

Optimal FFR-A Allocation

This chapter describes the method designed for choosing which FRR-A bids to activate. The objective is to autonomously activate the cheapest bids as long as there is capacity available. Since power experiences loss when transferred, the distance between the activated generator and the demand can be minimized as an ancillary goal. This, and other factors, will be used as tiebreakers for deciding between bids of equal price.

4.1 Control Center

A centralized solution is proposed, where an FRR-A Control Center receives demands from the AGC in each area. The total demand for all the whole power system is then met by activating FRR-A bids from different GENCOs, thus restoring the frequency. The interaction between control areas and the Control Center is shown in Figure 4.1 and a Simulink block diagram of the Control Center is shown in Figure 4.2.

The Control Center is implemented as a separate Simulink block, shown in Figure 4.2. The overall control strategy is set in the Control Center Simulink block, so the different control strategies can be compared in the results.

- *No AGC*: No secondary control loop, only primary control. $\Delta P_{m,d} = 0$.
- *Standard AGC*: Demand from AGCs are fed straight back to control areas as $\Delta P_{m,d}$ and desired tie-line flows are set to zero ($\Delta P_{tie,d} = 0$).
- *Optimal FRR-A Allocation*: Demands from AGCs are accounted for in a MILP problem, minimizing costs and constrained by tie-line capacities. $\Delta P_{m,d}$ contains the setpoints for activated FRR-A and $\Delta P_{tie,d}$ is the predicted flow. As the algorithm handles FRR-A bids in megawatts and the local states are in *per-unit*, all inputs are multiplied with P_{base} and the outputs are divided by P_{base}.

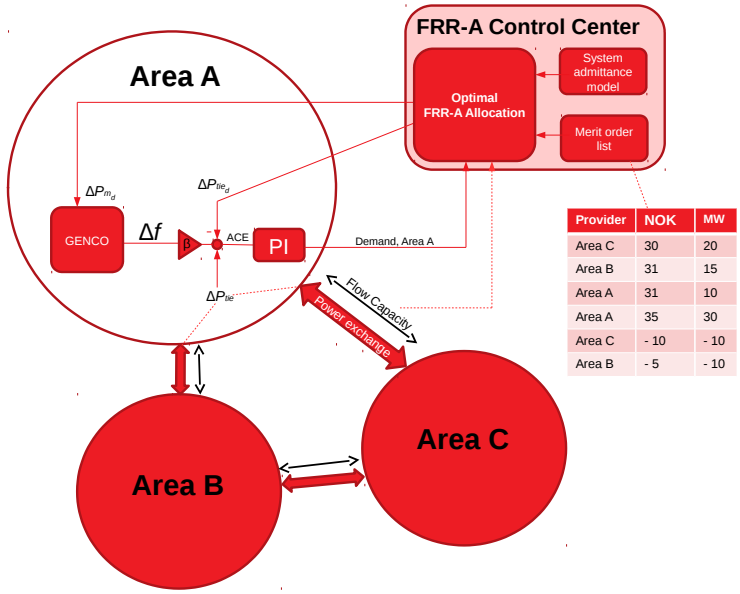

Figure 4.1: Interaction between the FRR-A Control Center and control areas. The output of the local AGCs are sent to the Control Center as demands. The Control Center then decides where to activate FRR-A and does so by setting $\Delta P_{m,d}$ for the primary loops. The Control Center also sets the desired flow, $\Delta P_{tie,d}$ in the local ACE calculations.

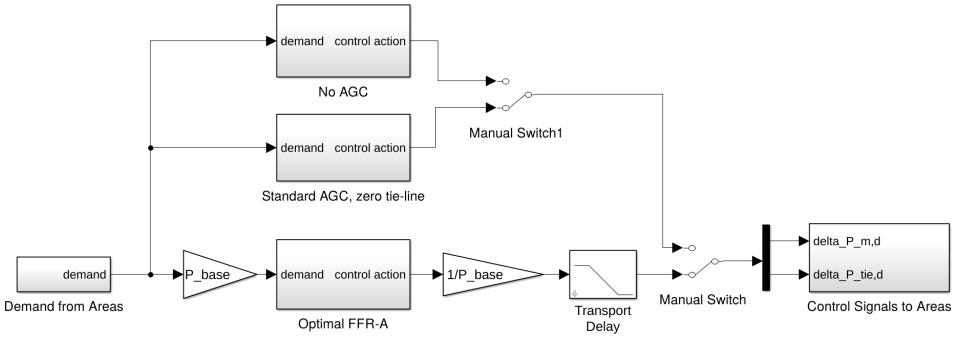

Figure 4.2: Simulink diagram of Control Center. Three different control strategies can be selected with manual switches.

4.2 Optimal FRR-A Allocation

The objective of the algorithm is to reduce FRR-A cost while providing setpoints ($\Delta P_{m,d}$ and $\Delta P_{tie,d}$) that are within *available transmission capacity* (ATC). In order to ensure that activation of the secondary reserves will not cause tie-lines to exceed ATC, the flow is predicted with DC load flow approximation. The optimal FRR-A allocation has a sample time of 10 seconds and the optimization time must therefore be less than that. A first order filter low-pass filter with a 60 seconds time constant is added to the output of the optimal FRR-A allocation to simulate the 120 second activation delay from GENCOs.

4.2.1 FRR-A Bids

The optimization algorithm uses lists of FRR-A bids as one of its inputs and the structure of the bid list is shown in Figure 4.1. One bid consists of three elements: The area providing the reserve, the quantity in megawatts and the price in NOK per megawatt. A positive quantity means that production will be up-regulated, while a negative quantity means that production will be down-regulated. The total cost for the TSO of activating bid i in NOK is $FRRA_{cost,i} = c_i|Q_i|$, where c is the bid price per megawatt and Q is the bid quantity in megawatt. Note that the price is multiplied with the absolute value of the quantity. A positive price means that the TSO will pay the GENCO for the effect of the bid to happen, while a negative price means that the GENCO pays the TSO. This is different from the current practice for FFR-A bids at Statnett. The change is done so that both UP and DOWN bids may be merged together as one bid matrix in the optimization problem.

As there currently does not exist an hourly market for FRR-A in the Nordic region, example bid lists generated by Statnett are used for testing the allocation algorithm. The example bid list is for hour 8 on the 02.06.2014 consists of 206 UP-bids and 320 DOWN-bids. The 120 first (and most relevant) bids are listed in Appendix C. The prices and quantities are fictional and not necessary scaled correctly. The result should therefore focus on the concept of the optimization and not on the actual values. Total FRR-A cost in NOK will however be presented, in order to compare different scenarios and optimization tunings. The FRR-A cost in NOK is also a good base for the optimization objective value.

The power system consists of n areas and has i branches. The bid lists are converted into bid matrices using *generateBidMat.m* shown in Appendix A. $\boldsymbol{Q}_{min}$ and $\boldsymbol{Q}_{max}$ represents the quantities and $\boldsymbol{C}$ represents the price. All the bid matrices are in $\mathbb{R}^{n\times m}$, where m is the number of bids for the area with the most bids. Both UP and DOWN versions of all matrices are necessary in order to restrict the optimization to only use up-bids when the total demand is positive, and only use down-bids when the total demand is negative.

4.2.2 Optimization Problem

The optimization problem is implemented as a MATLAB function block *allocateFRRA* with inputs and outputs to Simulink and is shown in 7.2 in Appendix B. The inputs to the function block need further explanation:

- demand: n-dimensional vector of the estimated demands from control areas.
- $\boldsymbol{Q}$ matrices: bid quantity matrices described earlier.
- $\boldsymbol{C}$ matrices: bid price matrices described earlier.
- $\boldsymbol{B_{prime}}$ and $\boldsymbol{D}$: Admittance matrices described in Chapter 2.
- $\boldsymbol{A}$ - Adjacency matrix described in Chapter 2.
- minFlowVector - m-dimensional vector with negative elements describing the minimum capacity of each tie-line.
- maxFlowVector - m-dimensional vector with positive elements describing the maximum capacity of each tie-line.
- flowCost - one-dimensional penalty constant for tie-line flow.
- activationCost - one-dimensional penalty constant for bid activations.

These values are then formulated into constraints and objectives, and passed into the YALMIP framework, as shown in the MATLAB script in Appendix A. The optimization variables are the voltage phasor angles of the control areas, $\vec{\theta} \in \mathbb{R}^{n \times 1}$ and the activated bid quantities, $\boldsymbol{P}_{bids} \in \mathbb{R}^{n \times m}$. Help variables are introduced: $\vec{P}$ is the total nodal injection at each area, or total FRR-A area production minus the demand in the area and is defined in Eq. (2.6). The flow vector, $\vec{P_{flow}}$, is defined in Eq. (2.6).

Constraints

The following constraints are set in the optimization problem:

- The sum of activated FRR-A must equal the total demand: sum of all elements in $\boldsymbol{P}_{bids}$ = sum of demands.
- Activated FRR-A must be within bids: $\boldsymbol{Q}_{min} \leq \boldsymbol{P}_{bids} \leq \boldsymbol{Q}_{max}$
- DC load flow approximation - find voltage phasor angles: $\vec{P} = \boldsymbol{B'}\vec{\theta}$
- DC load flow approximation - find flow: $\vec{P_{flow}} = \boldsymbol{DA\theta}$
- Flow within ATC: *minFlowVector* $\leq \vec{P_{flow}} \leq$ *maxFlowVector*

Objective Function

The following costs are minimized in the optimization problem:

- FRR-A cost: activated FRR-A bids multiplied by the price of that bid
- Flow cost: total tie-line flow multiplied by the *flowCost* constant
- Activation cost: number of activated bids multiplied by the *activationCost* constant

Mixed Integer Linear Program

The activation cost is implemented by multiplying binary *onoff* variables with each bid and adding a small activation cost in the objective function. The number of activated bids is an integer objective, making the optimization problem a mixed integer linear program (MILP). As the TSO needs to activate FRR-A from different generation companies, it makes sense to activate as few as possible, if the bid-prices and transmission costs are identical. Without it, the solver may activate small fractions of several bids with the same total cost. More importantly, it is of interest to simulate the optimization as a MILP as practical issues in an implementation may be formulated as integer constraints or objectives.

Best Effort Solution

When there are not enough FRR-A bids to cover the total demand, or the FRR-A bids do not provide a solution that does not exceed ATC, the optimization should fail the best possible way. A best-effort MILP problem is therefore defined and is executed if the original MILP problem fails to find a feasible solution. The tie-line flow constraint is still kept as a hard constraint, but a slack variable, $\vec{P}_{slack} \in \mathbb{R}^{n\times 1}$, is added to the constraint $\vec{P} + \vec{P}_{slack} = \boldsymbol{B'}\vec{\theta}$. The slack variable is then penalized in the objective function by multiplying it with a constant *prodSlackCost* $= 100000$ and summing the vector. As long as this constant is high enough, it will penalize the use of the slack variable so much that it will not be used unless no other feasible solution exists.

4.2.3 Optimization Solver

Framework: YALMIP

For setting up and solving the optimization problem, YALMIP (Löfberg, 2004) release 20150918, is used. YALMIP is a modelling language for advanced modelling and solution of convex and non-convex optimization problems. It is implemented as a free toolbox for MATLAB. It allows the user to set up an optimization problem, and YALMIP takes care of the low-level modelling to obtain efficient and numerically sound models. YALMIP identifies the type of optimization problem, models it in a form suitable for solvers, while the actual solving is done by external solvers.

Solver: IBM-CPLEX

The IBM ILOG CPLEX solver (IBM, 2016) will be used to solve the MILP optimization problem. It uses an LP-based branch and bound algorithm combined with cutting plane techniques and is considered one of the best solvers on the market for solving MILPs (Méndez et al., 2006).

Solver: MATLAB INTLINPROG

INTLINPROG (Matworks, 2016) is part of the commercial Optimization Toolbox from MATLAB R2014a. It will be tested and compared to the CPLEX solver.

Chapter 5

Simulation Results

The first section presents the response of the model with primary control and with *standard AGC*. More control areas are then added, showing how the ACE-calculations and *standard AGC* work. In Section 5.2, the optimal production allocation algorithm is introduced and the local AGC passes the output to the Control Center. All eleven control areas, reflecting the Nordic synchronous region, are simulated, featuring plots for total load disturbance and FRR-A production. Different scenarios are used to illustrate how the algorithm handles tie-line capacity problems, insufficient FRR-A bids and the addition transmission costs.

It is important to note that all states are deviations from the hourly market setpoints. The tie-line capacities are therefore the remaining transmission capacity, accounting for the hourly scheduled flow. As some tie-lines are already maximized from the power market trade, there will typically be no ATC in one direction, but plenty in the opposite direction. In practice, a tie-line flow in the simulations may therefore mean a decrease of flow.

Control areas are simulated with individual parameters given in Table 3.1. Frequencies are plotted as $f = f_N + \Delta f$ with orange and red dashed lines at 50 ± 0.05Hz and 50 ± 0.10Hz to get a more practical sense of the frequency and acceptable limits. As the frequencies in the Nordic system are quite synchronous they are plotted as one common frequency in some of the results.

5.1 Primary Response and Standard AGC

5.1.1 One Control Area

NO1 is simulated as an isolated control area without any tie-line connections to other areas. A disturbance of $\Delta P_L = 0.03pu = 75MW$ occurs after $t = 2s$, and the response of the generating unit is shown in Figure 5.1. With only primary control, the mechanical power, ΔP_m, has a slightly under-damped response and settles at the level of the disturbance in 150 seconds. The primary control has no feedback from the frequency, and the

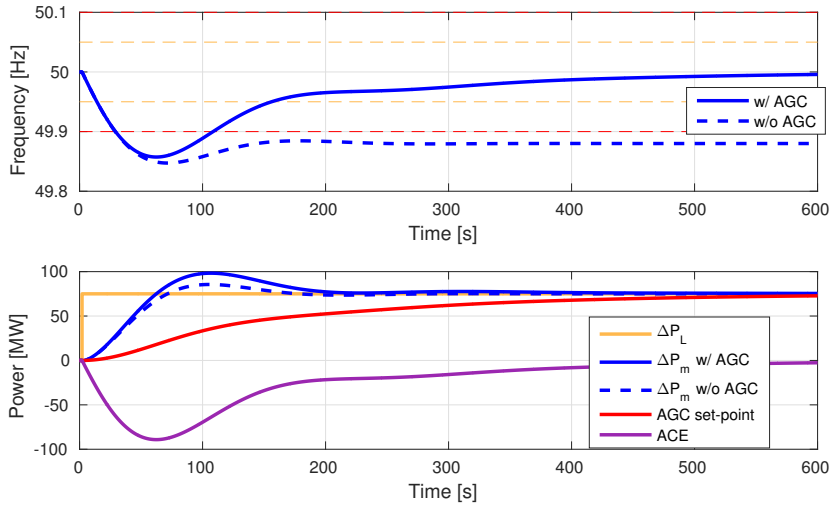

Figure 5.1: Step response for generating unit with only primary control (dashed lines) and with secondary control (solid lines). Load step $\Delta P_L = 0.03pu = 75MW$ at $t = 2s$

frequency stabilizes at $f = 49.88$Hz, giving a stationary error of $\Delta f = -0.12$Hz. According to (2.1) this corresponds to a droop of $\rho = \frac{\Delta f}{f_N \Delta P_m} = -0.08 = 8\%$. Due to the under-damped response, the frequency is slightly restored by the primary control action.

The secondary control uses the ACE signal to compute its control action. As there are no tie-line connections, the ACE signal is in this case only a function of the frequency error. As seen from the solid lines in Figure 5.1, the ACE reaches a little over -75MW before it is slowly brought back to zero by the secondary integral controller. The AGC setpoint is slowly increasing until it settles at 75MW. Due to the increased AGC setpoint, the primary governor produces a higher output and the mechanical power, ΔP_m, is increased. The frequency is within acceptable limits in 200 seconds. The secondary response is over-damped and settles with no overshoot.

5.1.2 Three Control Areas

Three control areas, NO1, NO2, and NO5, and their tie-line connections, $tieline_1 = NO1 - NO2$, $tieline_3 = NO1 - NO5$ and $tieline_5 = NO2 - NO5$, are simulated with the parameters from Table 3.1. Tie-line connections to other areas are disabled so that the total power system is reduced to these three areas. A load disturbance of $\Delta P_L = 0.06pu = 150MW$ occurs after $t = 2s$ in NO1. The response of the three areas with and without AGC is shown in Figure 5.2. The frequency is plotted as one common frequency for the three areas.

Without secondary control (AGC), the three areas contribute almost equally with primary

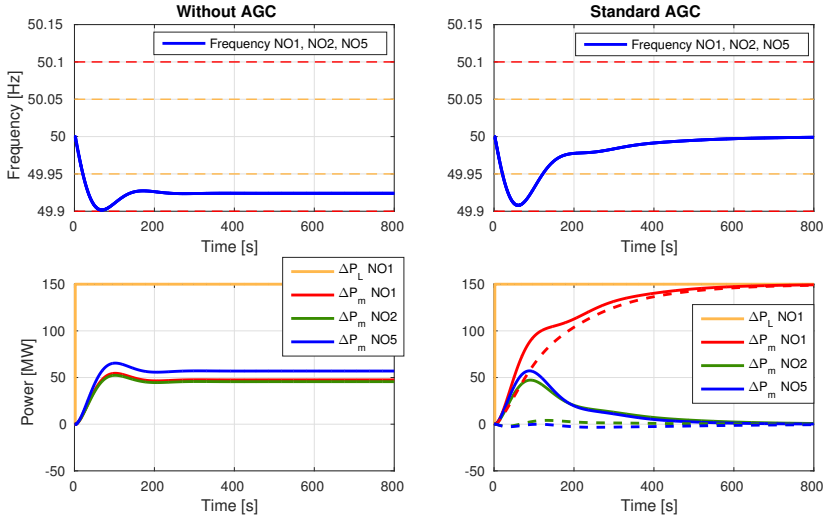

Figure 5.2: Step response for three interconnected areas, NO1, NO2 and NO5, with and without secondary control. The generator mechanical power change, ΔP_m, in the control areas are shown (solid lines) along with its AGC setpoints, ΔPm_d (dashed lines). Load step $\Delta P_L = 0.06pu = 150MW$ at $t = 2s$ in NO1

reserves and the frequency stabilizes at $f = 49.925$Hz. With standard AGC, the primary response is similar, but the AGC setpoint for NO1 restores the frequency and drives the production to NO1, where the load disturbance occurred. The primary control provides damping against the disturbance, while the secondary control restores the frequency to 50Hz and the tie-line exchange to zero.

5.2 Optimal FRR-A Allocation

The centralized optimal production allocation algorithm is now introduced and FRR-A bids are activated by a centralized Control Center. The local secondary controllers are as before, but instead of directly acting as the setpoint for the primary control loops, their outputs are directed to the Control Center. The local demands are summed up in the Control Center and the total demand is met by automatically activating FRR-A bids from the participating control areas.

5.2.1 Three Control Areas

Using the same power system and load disturbance as in Figure 5.2, the FRR-A allocation algorithm is applied with only FRR-A bids available from NO5. This means that the 100 MW demand in NO1 must be met in full by production from NO5. All tie-line capacities are in this simulation set to 1000 MW both ways for all three tie-lines in order to avoid

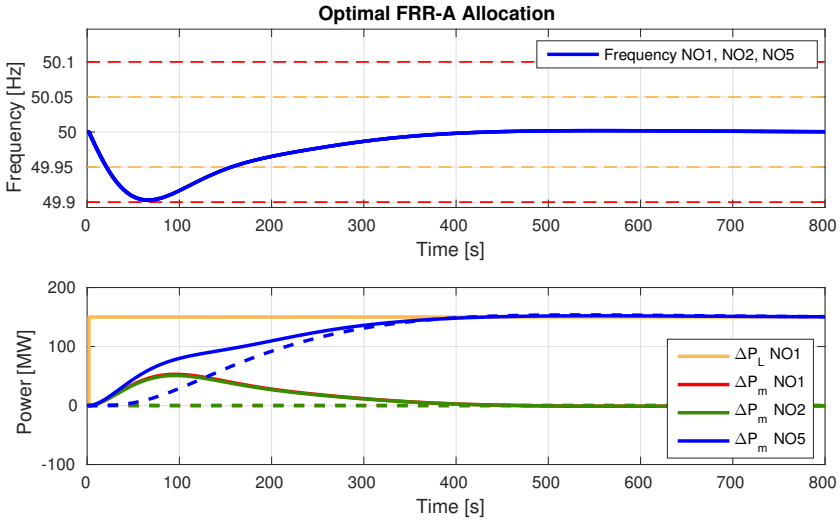

Figure 5.3: Step response for three interconnected areas, NO1, NO2 and NO5, with optimal FRR-A allocation. The generator mechanical power changes, ΔP_m, in the control areas are shown (solid lines) along with their setpoints, $\Delta P_{m,d}$, from the the Control Center (dashed lines). Load step $\Delta P_L = 0.06pu = 150MW$ at $t = 2s$ in NO1.

capacity constraints. The result is shown in Figure 5.3.

As with the standard AGC in Figure 5.2, the optimal FRR-A allocation is able to restore the frequency, but uses only secondary reserves that are available from the bid list. NO1 and NO2 produces up to 50MW from the primary control before the primary reserves are freed by the FRR-A in NO3. The setpoints for NO1 and NO5 remain at zero.

5.2.2 Nordic Synchronous Region

The whole synchronous region is simulated with full FRR-A bid lists available. Tie-line capacities are again is set high. Activated FRR-A, following a 200MW disturbance in SE3 is shown in Figure 5.4. The activated FRR-A is slowly increasing as the secondary controllers start to integrate the ACE. The cheapest bid from NO4 is fully activated after 150 seconds, and bids from NO2, NO5 and SE2 are then activated. The frequency is restored to 50 Hz and the total FRR-A settles at 200MW with FRR-A cost = 6690 NOK.

5.2.3 Infeasible Problem

The whole synchronous region simulated with a load disturbance of $\Delta P_L = 0.275pu = 687.5MW$ in NO1. No FRR-A is available (the bid list is empty), thus the optimization problem is infeasible and the best-effort solution is applied. The results are presented in Figure 5.5.

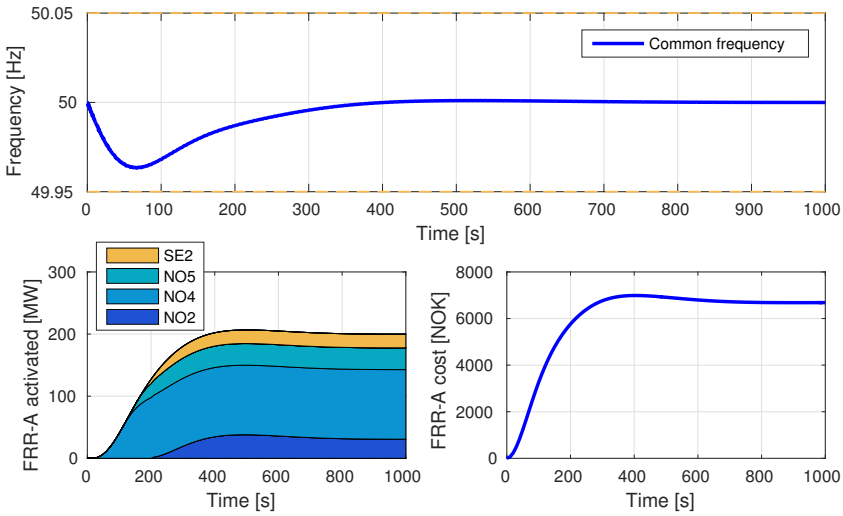

Figure 5.4: Optimal FRR-A Allocation: Nordic Synchronous Region

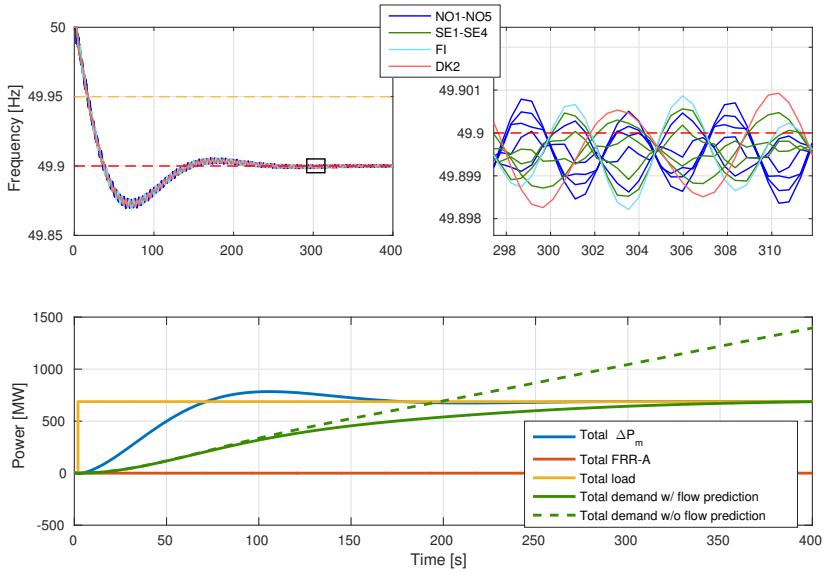

Figure 5.5: Response for the whole Nordic Synchronous region with load step $\Delta P_L = 0.275pu = 687.5MW$ at $t = 2s$ in NO1. The total demand, estimated by the local secondary controllers, is shown in green in the bottom plot.

The primary response settles at the level of the disturbance after 150 seconds and the frequency stabilizes at $\Delta f = -0.1$Hz. This corresponds to a total droop of $\rho_{tot} = \frac{\Delta f}{f_N} \frac{11 \cdot 2500MW}{687.5MW} = 0.08$. All 11 local frequencies are plotted, with a separate plot zoomed in to show the frequency oscillations. It can be seen that the frequencies have small oscillations with frequency of 0.3 to 0.5Hz.

As shown in the dotted green line, the demand from the local secondary controllers continues to grow when the systems settles at a state where the ACE is non-zero. The predicted flow from the best-effort FRR-A allocation ΔP_{tie_d}, is subtracted in the ACE calculations. This makes the ACE converge to zero and the estimated demand therefore converges to the level of the disturbance, as seen from the solid green line. This prevents wind-up of the AGCs when the system stays at a non-ideal state for a long period of time.

5.2.4 Load Ramp

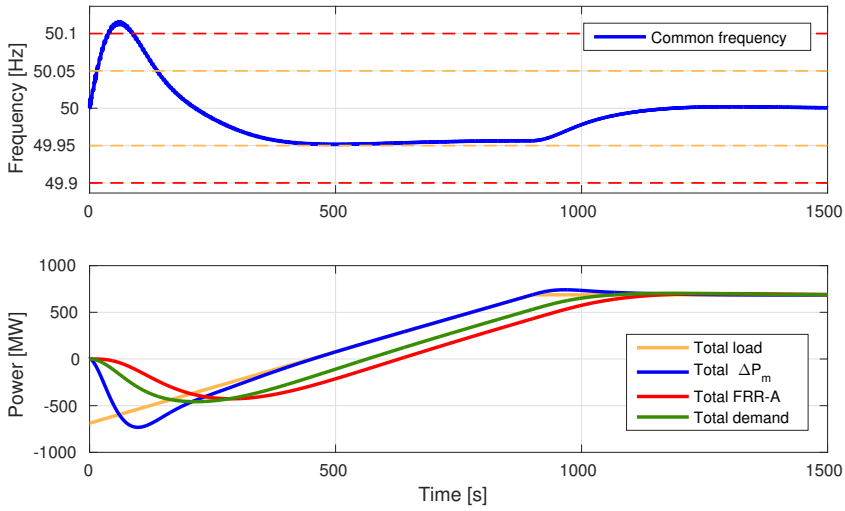

Figure 5.6: Response for the whole Nordic Synchronous region with a load ramp in NO1.

Figure 5.6 shows the synchronous region exposed to a load ramp. The load disturbance starts at -680MW and settles at 680MW after 900 seconds. The Control Center has sufficient secondary reserves available and no tie-lines have strict capacity limits. The total estimated demand (green line) settles at stationary error from the actual load (yellow line) during the ramp. The total FFR-A production is lagging the demand with about 70 seconds due to the FRR-A activation delay. After the ramp, the demand and FRR-A settles at 680MW without any overshoot.

5.2.5 Optimization

The optimal FRR-A allocation algorithm is tested for special cases and optimization penalties are varied. Full bid lists for UP and DOWN FRR-A are used. A 200MW demand exists in SE3 and the demand is covered from activating different bids, depending on different constraints and objective penalties. Since the total demand is positive, only the UP-bids are used, except in Case 5 where both UP and DOWN bids are included. To show the capacity constraint in an orderly fashion, one tie-line, NO1-SE3, has been focused on in these results. Case 1 is used as a base case. The optimization is solved both with the IBM-CPLEX solver and with the MATLAB built-in solver INTLINPROG and the optimization times are presented for each case. The Yalmip set-up time is also presented.

FRR-A cost	6690.20 NOK
Clog cost	0.4556
Activation cost	7
Total cost	6697.7
Yalmip time	1323 ms
CPLEX	68 ms
INTLINPROG	455 ms
Flow NO1-SE3	91.3 MW
Activated FRR-A Bids Area: [MW]-[NOK]	NO4: 112 - 33.09 NO5: 11 - 33.09 NO5: 24 - 33.68 SE2: 12 - 33.95 SE2: 10 - 34.20 NO2: 18 - 34.27 NO2: 13 - 34.27

Table 5.1: Case 1: Normal operation

FRR-A cost	6821.00 NOK
Clog cost	0.5128
Activation cost	300
Total cost	7121.5
Yalmip time	1463 ms
CPLEX	107 ms
INTLINPROG	303 ms
Flow NO1-SE3	96.8 MW
Activated FRR-A Bids Area: [MW]-[NOK]	NO4: 112 - 33.09 NO5: 24 - 33.68 NO5: 64 - 36.04

Table 5.2: Case 2: Activation cost: 100

Case 1: Normal Operation

All tie-line capacities are set to [-1000, 1000] to ensure no capacity problems. The FRR-A objective value is simply the cost of the secondary reserves activated. Activation cost is set to 1 and Flow cost is set to 0.001. The results are shown in Table 5.1. Figure 5.4 shows the the same conditions simulated on the power system.

As there are no capacity concerns and the only major cost contributing to the objective value is the FRR-A cost, the cheapest bids from the whole synchronous region are chosen with a total of 6690 NOK. The low activation cost only acts in on the result when there are multiple bids with equal price. There are 3 bids of equal price from NO2, but since two of will cover the demand, the third is not activated at all. The total predicted flow is $\frac{0.4556}{0.001} = 455.6MW$ (sum of all flows on all tie-lines).

Case 2: High Activation Penalty

Constraints and objective are set identical to Case 1, with the exception of Activation penalty = 100. The results are shown in Table 5.2.

Penalization of the activated bids reduces the number of activated bids from 7 to 3 bids by forcing the MILP to choose bids with large quantities. The FRR-A cost is increased with 132 NOK from Case 1.

FRR-A cost	7818.40 NOK
Clog cost	1060
Activation cost	12
Total cost	8890.4
Yalmip time	1325 ms
CPLEX	86 ms
INTLINPROG	362 ms
Flow NO1-SE3	37.7 MW
Activated FRR-A Bids Area: [MW]-[NOK]	NO5: 11 - 33.09 NO5: 2 - 33.68 SE2: 12 - 33.95 SE2: 10 - 34.20 NO2: 8.66 - 34.27 NO1:16 - 36.04 SE2: 20 - 37.35 SE3: 65 - 38.00 SE4: 0.33 - 41.88 SE3: 10 - 43.00 SE3: 30 - 44.40 SE3: 15 - 51.40

Table 5.3: Case 3: Flow cost: 10

FRR-A cost	9828.00 NOK
Clog cost	0.1541
Activation cost	12
Total cost	9840.2
Yalmip time	1336 ms
CPLEX	79 ms
INTLINPROG	271 ms
Flow NO1-SE3	5.0 MW
Activated FRR-A Bids Area: [MW]-[NOK]	SE2: 12 - 33.95 SE2: 4.2 - 34.2 SE3: 65 - 38.00 SE4: 5 - 41.88 SE3: 10 - 43.00 SE3: 30 - 44.40 SE3: 15 - 51.40 DK2:16 - 60.3 DK2: 11 - 62.31 DK2: 10 - 71.03 DK2: 11 - 76.12 DK2: 10.8 - 80.41

Table 5.4: Case 4: Max flow NO1-SE3: 5MW

Case 3: High Flow Penalty

Constraints and objective are set identical to Case 1, with the exception of Flow cost = 100. The results are shown in Table 5.3.

Penalizing the tie-line flows reduces the total power exchange in the network and forces the MILP to activate secondary reserves close to the disturbance. No reserves from the cheapest bid in NO4 are activated due to the long transmission distance. More expensive bids in SE3 and neighbouring areas are activated instead. A total of 120MW is activated in SE3, while 58.33MW comes from adjacent areas and 21.66MW from areas with two tie-lines in between. The total flow in the network is reduced by $350MW$ and the FRR-A cost is increased with 1128 NOK compared to Case 1.

Case 4: Max Tie-Line Capacity

Constraints and objective are set identical to Case 1, but with a tie-line max capacity of 5MW on the NO1-SE3 tie-line. The results are shown in Table 5.4.

The hard constraint of the maximum flow is withheld at a FRR-A cost of 3138 NOK more than Case 1. To keep the flow at NO1-SE3 under 5MW, all reserves are activated in Sweden and DK2. Especially the reserves in DK2, SE4 and SE3 are favourable in this case, as production in those areas will not contribute at all to the flow from NO1 to SE3.

The conditions in Case 4 are simulated on the power system model and the result is shown in Figure 5.7, with a few adjustments: Initially, only the first FRR-A bid (112MW in NO4) is available. This causes the optimization problem to become infeasible, and the best-effort problem is solved. Only about 25MW is activated in NO4 as more would cause the predicted NO1-SE3 flow to exceed the 5MW limit. Frequency is therefore not restored. After 400 seconds, all bids are made available, and the optimization finds a solution (Table 5.4) that both restores the frequency and is within ATC. Notice that the activated FRR-A increases to 200MW quickly after all bids are made available: As shown in Figure 5.5, the demand is converging to the load disturbance due to the $\Delta P_{tie,d}$ values of the best-effort solution. When the bids become available, the FRR-A allocation immediately activates the bids, and the only delay is the 120 second activation delay implemented as a first order filter. The frequency is then restored and the NO1-SE3 flow is brought down to 5MW. As NO1 neighbours SE3, where the disturbance occurred, the initial tie-line flow reaches almost 80MW. The primary control loop has no feedback on the tie-lines flow and the the optimal FRR-A allocation has no reserves to activate that would bring the flow down to under 5MW.

Case 5: Using both UP and DOWN bids

Constraints and objective are set identical to Case 1, but the optimization has access to both UP-bids and DOWN-bids. The results are shown in Table 5.5.

The total demand of 200MW is covered by up-regulating with a total of 214MW and down-regulating with 14MW in DK2. When the 200MW demand is covered, there are still cheaper UP-bids than the income of the DOWN-bid from DK2, and 14MW is activated both up and down in parallel. After that, the next favourable DOWN-bid is in FI at -35.00 NOK, which is not enough to compensate for buying more from NO2 at 35.45 NOK.

The conditions in Case 5 are simulated on the power system model and is shown in Figure 5.8. The response of the frequency is similar to Figure 5.4 where no DOWN bids are available, but the FRR-A cost is reduced. Initially, the bid with negative price in FI is activated, but when the demand becomes high enough, it is not profitable. Note that the DOWN bid in FI is activated, even though the frequency is $\Delta f = -0.035$Hz. The 14MW bid in DK2 is kept in the steady state solution.

FRR-A cost	5794.00 NOK
Flow penalty	0.5185
Activation penalty	10
Objective Value	5804.5
Yalmip set-up	2290 ms
CPLEX	86 ms
INTLINPROG	265 ms
Flow NO1-SE3	100.4 MW
Activated FRR-A Bids Area: [MW]-[NOK]	NO5: 11 - 33.09 NO4: 112 - 33.09 NO5: 24 - 33.68 SE2: 12 - 33.95 SE2: 10 - 34.20 NO2: 20 - 34.27 NO2: 13 - 34.27 NO2: 10 - 34.27 NO5: 2 - 35.45 DK2: (-14) - (-98.45)

Table 5.5: Case 5: DOWN-bids available

Optimization Time

The Yalmip set-up time is the most time consuming, using around 13500 ms on average and 2290 ms when DOWN-bids are included in Case 5. CPLEX solves the MILP in 85 ms on average while INTLINSOLVE uses 292 ms. Neither of the solver times increased in Case 5, where 320 more bids are added to the problem, more than doubling the size of the problem.

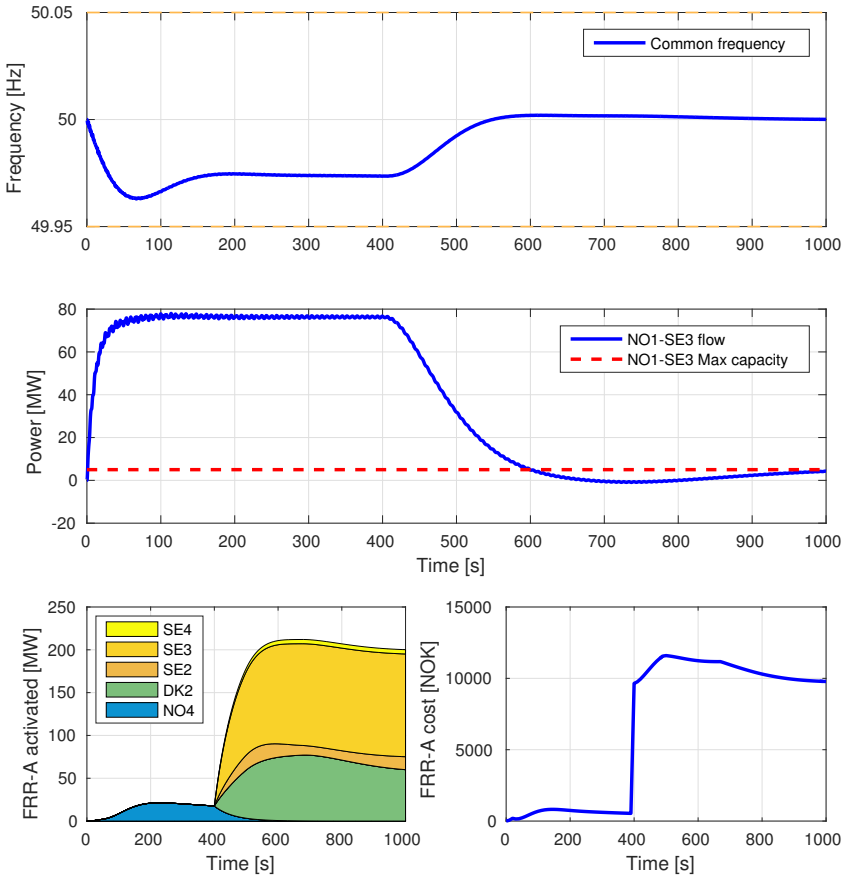

Figure 5.7: Optimal FRR-A Allocation: Case 4

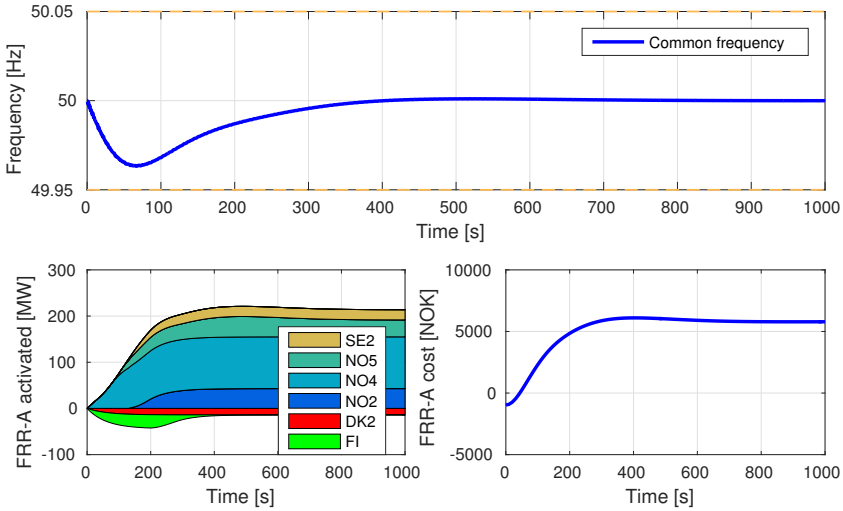

Figure 5.8: Optimal FRR-A Allocation: Case 5

Chapter 6

Discussion

6.1 Power System Model

The model developed to test the control strategy mostly concerns the primary response and is therefore only briefly discussed in this section.

6.1.1 Control Area Model and Primary Control

The simulation results show that the primary control has the desired response and the desired droop of the whole system's primary response of 8% is achieved. The power exchange between areas is fast, with oscillations around 0.5Hz, giving the local frequencies the same oscillation. This causes almost identical frequencies for the whole synchronous region, which matches the behaviour of the Nordic power system.

6.1.2 Secondary Control

The standard AGC works as expected for one control area and for three interconnected control areas. It brings the ACE to zero, meaning both the frequency and tie-line flows are as desired. The response is quite slow, and could be tuned up for the standard AGC tests. However, the integrator constant, T_i, is kept at 200 seconds, to be able to cope with the delays that occur in the further tests with a centralized Control Center.

6.2 Optimal FRR-A Allocation

The overall control structure and the optimization algorithm is discussed in this section.

6.2.1 Centralized Allocation

The centralized solution has the benefit that it knows all the states, which in this case are local demands, a model of the system admittances and all available FRR-A bids. This

makes it possible to find the global optimal solution. The upsides and downsides to a centralized versus a decentralized solution are summarized:

+ Requires no communication between control areas
+ Only control area demands are sent to the Control Center
+ The centralized solution has defined in- and outputs and the algorithm can be completely changed with the same interaction between control areas and Control Center.
+ The objective function penalties can easily be adjusted to achieve different behaviour.
− Requires a model of admittances of all tie-lines.
− One large optimization problem.
− Adding new control areas changes the structure of the optimization problem.

As mention in (Venkat et al., 2008), the downside of having one large optimization problem is that computation time becomes too great. This is avoided by using a linear model of the power flow and keeping other constraints and objectives linear. To make the solution highly scalable and module based a completely distributed control structure can be researched, where each control area only knows its own state and the state of its tie-line connection. This will allow for plug-and-play of new areas. By adopting a decentralized solution to the DC load flow (mentioned Section 1.2 and decentralizing the bid system, the centralized approach proposed in this thesis can be decentralized.

6.2.2 Objective Function

The optimization works as a compromise between economical aspects and the state of the power system, from activating only the cheapest bids, to activating reserves in the same area as the disturbance.

The results show that the objective function penalties work as expected, and shows how penalizing certain states can be used to compromise between FRR-A cost and the state of the power system. The penalties used in the 5 different cases are exaggerated and the results should only be considered as conceptual.

In the optimization, the cost penalty is the same for both flow directions of the tie-lines. As mentioned in the results, a flow in one direction may actually mean a decrease in the total flow, when the hourly scheduled flow is accounted for. The flow penalty should therefore be negative in one of the flow directions. This can be achieved with the FRR-A allocation algorithm knowing the actual flow on the tie-lines, instead of operating with deviations from the hourly setpoints.

An important restriction of the FRR-A allocation is the fact that it only sends out setpoints to the local areas. The only feedback from the areas are the estimated demands, and the centralized algorithm has no way of guaranteeing that the tie-line flows are within

limits. Since the secondary controllers have a time constant of $T_i = 200$ seconds, the Control Center does not cope with fast dynamics between the areas, and only the steady state is guaranteed to converge to a state with acceptable tie-line flows.

The result from using both UP and DOWN works in theory, but are not realistic. Bids that give a surplus to activate in parallel are not very likely to occur. Up and down-regulation in parallel may also aggravate the frequency error. If up- and down-bids, that are profitable to activate in parallel, do exist and the system is already in a good state, activating both may be an option. A good state means that the frequency is at 50Hz, lots of reserves are available and tie-lines are well within limits. Parallel activation can cut expenses for the TSO, and help out two GENCOs where one desperately needs to down-regulate and the other wants to up-regulate. The proposed optimal FRR-A allocation algorithm is, however, not suited for making such decisions as it is.

6.2.3 Flow Prediction

The main assumptions for the power network in the allocation algorithm is the DC load flow approximation. The accuracy of the approximation is however not validated in this thesis, as the simulation model of the power network is modelled with the same approximation. The only errors from the prediction model to the actual model are the difference in admittance values. The FRR-A allocation algorithm needs to be further tested on a more complex model of the Nordic power system. If the DC load flow turns out to be too inaccurate, a more advanced prediction of the power flow can implemented, increasing the complexity of the optimization problem. However, the flow prediction is also dependent on the estimated demands from secondary controllers. This demand is used as an approximation of the load disturbance in each area. As seen in the results, the estimated demand does converge to the load disturbance, but before a steady state is reached, the demand estimation may not be a good approximation of the load. As the estimated demand is not an accurate representation for the local load disturbance, it may not help to improve the power flow prediction model.

The feedback in the secondary controllers is the total flow out of the area, and not the flow of separate tie-line connections. The secondary controllers will therefore ensure that the total tie-line flow, ΔP_{tie}, is kept as set by the Control Center, while the distribution onto the different tie-lines is not measured and fed back in any way. Error in the admittance model may therefore cause power flows on each tie-line to differ somewhat from the predicted flow which could lead to flows exceeding maximum capacities.

6.2.4 Optimization Time

The simulation results show that the FRR-A setpoints are stable with a sampling time of 10 seconds. CPLEX solves the MILP in less than 0.2 seconds, which is well within the specification. Even the built-in solver in MATLAB, INTLINPROG solves the MILP in under 0.5 seconds yielding the same result as CPLEX. This makes it possible to reduce the

sample time of the FRR-A allocating algorithm if needed.

The slowest part of the algorithm, the Yalmip set-up time, can be ignored as this only needs to be done to set-up the MILP. As the only real-time inputs to the optimization are the local demands, the size and structure of the optimization remains the same, and the MILP only needs to be set up once. The admittances of the system and objective penalties may also be changed in real-time, as they do not change the structure of the problem. Allowing the FRR-A bid lists change dynamically would essentially change the size of the MILP and it would have to be set up for each optimization. This can be avoided by setting a maximum size and filling the empty entries with zero bids. The problem can also be reduced in size by pre-processing the bids and removing unrealistic bids: If there exists low priced bids of large quantities in an area, the more expensive bids can be removed as they would never get activated. This could be valuable if non-linear constraints or costs are added to the optimization problem.

Chapter 7

Conclusion

An alternative control structure to current FRR-A regulation has been proposed and tested. A solution combining area based secondary controllers and a centralized allocation algorithm is implemented and simulated on a linear model of a power system. A module-based simulator of control areas is implemented in Simulink, where control strategies can be selected in a centralized Control Center. The module-based design allows for new control strategies to be tested, or the power system model to be changed.

FRR-A is successfully activated as cheaply as possible, based on FRR-A bids from GENCOs and constrained by tie-line capacities. Different penalization of the optimization problem is presented, showing the affect on the solution. The MILP problem is solved in under 0.2 seconds for 11 control areas and 526 FRR-A bids, using the IBM CPLEX solver. This is within the speed requirements, and the optimization time does not increase mentionably when adding more control areas or bids.

The DC flow method quickly predicts power flow and makes the secondary controllers converge to the local load disturbance, thus working as a demand estimator. This is dependent on the accuracy of the admittance model used in the prediction. As the power flow prediction uses the same approximation method as the simulated model, the prediction will yield unrealisticly accurate values. The suggested control strategy should therefore be tested on a more complex and realistic model of the Nordic power system.

A centralized solution may be a good option for the Nordic region at the moment, but as the power network is evolving to a more distributed nature, a distributed control structure should be researched further.

Bibliography

Åström, K. J., Hägglund, T., 2006. Advanced PID control. ISA-The Instrumentation, Systems, and Automation Society; Research Triangle Park, NC 27709.

Bakirtzis, A., Biskas, P., 2002. Decentralised dc load flow and applications to transmission management. In: Generation, Transmission and Distribution, IEE Proceedings-. Vol. 149. IET, pp. 600–606.

Bakirtzis, A. G., Biskas, P. N., 2003. A decentralized solution to the dc-opf of interconnected power systems. Power Systems, IEEE Transactions on 18 (3), 1007–1013.

Balchen, J., Andresen, T., Foss, B., 2003. Reguleringsteknikk Department of Engineering Cybernetics.

Beaufays, F., Abdel-Magid, Y., Widrow, B., 1994. Application of neural networks to load-frequency control in power systems. Neural Networks 7 (1), 183–194.

Bénichou, M., Gauthier, J.-M., Girodet, P., Hentges, G., Ribière, G., Vincent, O., 1971. Experiments in mixed-integer linear programming. Mathematical Programming 1 (1), 76–94.

Bevrani, H., 2014. Robust Power System Frequency Control. Springer.

Bixby, E. R., Fenelon, M., Gu, Z., Rothberg, E., Wunderling, R., 2000. Mip: Theory and practice—closing the gap. In: System modelling and optimization. Springer, pp. 19–49.

Chaudhuri, N. R., Domahidi, A., Majumder, R., Chaudhuri, B., Korba, P., Ray, S., Uhlen, K., 2010. Wide-area power oscillation damping control in nordic equivalent system. Generation, Transmission & Distribution, IET 4 (10), 1139–1150.

Conejo, A. J., Aguado, J. A., 1998. Multi-area coordinated decentralized dc optimal power flow. Power Systems, IEEE Transactions on 13 (4), 1272–1278.

Eivind Lindeberg, S., 2014. Automatisk frekvensregulering i det nordiske kraftnettet. Tech. rep.

Ersdal, A. M., Imsland, L., Uhlen, K., 2015a. Model predictive load-frequency control.

Ersdal, A. M., Imsland, L., Uhlen, K., Fabozzi, D., Thornhill, N. F., 2015b. Model predictive load–frequency control taking into account imbalance uncertainty. Control Engineering Practice.

Glover, J. D., Sarma, M., Overbye, T., 2011. Power System Analysis & Design, SI Version. Cengage Learning.

IBM, 2016. CPLEX. http://www.ilog.com/products/cplex.

Knudsen, B., September 2015. *MILP algorithms: branch-and-bound and branch-and-cut*, "Lecture notes for the course TTK16 Mixed integer optimization in energy and oil and gas systems at NTNU (Accessed: 09.05.2016).

Löfberg, J., 2004. Yalmip: A toolbox for modeling and optimization in matlab. In: Computer Aided Control Systems Design, 2004 IEEE International Symposium on. IEEE, pp. 284–289.

Matworks, 2016. INTLINPROG. http://se.mathworks.com/products/optimization/features.html#mixed-integer-linear-programming.

McCalley, J., August 2012. *The DC Power Flow Equations*, "Lecture notes for the course EE 554 Steady-state analysis, Iowa State University" (Accessed: 15.04.2016).

Méndez, C. A., Cerdá, J., Grossmann, I. E., Harjunkoski, I., Fahl, M., 2006. State-of-the-art review of optimization methods for short-term scheduling of batch processes. Computers & Chemical Engineering 30 (6), 913–946.

Mohamed, T., Bevrani, H., Hassan, A., Hiyama, T., 2011. Decentralized model predictive based load frequency control in an interconnected power system. Energy Conversion and Management 52 (2), 1208–1214.

Nocedal, J., Wright, S., 2006. Numerical optimization. Springer Science & Business Media.

Pochet, Y., Wolsey, L. A., 2006. Production planning by mixed integer programming. Springer Science & Business Media.

Scattolini, R., 2009. Architectures for distributed and hierarchical model predictive control–a review. Journal of Process Control 19 (5), 723–731.

Schavemaker, P., Van Der Sluis, L., 2008. Electrical power system essentials. John Wiley & Sons.

Shayeghi, H., Shayanfar, H., Jalili, A., 2009. Load frequency control strategies: A state-of-the-art survey for the researcher. Energy Conversion and management 50 (2), 344–353.

Statkraft, 2016. 1000 MW wind power in Central–Norway. http://www.statkraft.com/about-statkraft/Projects/norway/fosen/, accessed: 02.06.2016.

Statnett SF, 2012a. Funksjonskrav i kraftsystemet 2012. Tech. rep.

Statnett SF, January 2012b. Technical agc interface specification for delivery of frequency restoration reserves to statnett. Tech. rep.

Statnett SF, January 2012c. Technical product specification for delivery of frequency restoration reserves to statnett. Tech. rep.

Statnett SF, February 2014. Systemdrifts- og markedsutviklingsplan 2014-20. Tech. rep.

Statnett SF, 2015. Halvårsrapport fra landssentralen. Tech. rep.

Statnett SF, 2016. NordLink. http://www.statnett.no/Nettutvikling/NORDLINK, accessed: 02.06.2016.

Uhlen, K., November 2015. *DC Power Flow and DC OPF*, lecture notes for the course TET4115 Power System Analysis, Norwegian University of Science and Technology.

Venkat, A. N., Hiskens, I. A., Rawlings, J. B., Wright, S. J., 2008. Distributed mpc strategies with application to power system automatic generation control. Control Systems Technology, IEEE Transactions on 16 (6), 1192–1206.

www.statnett.no, 2016. Nordisk produksjon og forbruk. http://statnett.no/Drift-og-marked/Data-fra-kraftsystemet/Nordisk-produksjon-og-forbruk/, accessed: 24.05.2016.

Appendices

A MATLAB Scripts

```
%% Generate bid matrices function
function [Q_min, Q_max, C] = generateBidMat(bidList, N)
    bids = zeros(1,N);
    [n_bids, ~] = size(bidList);
    % Count bids from each area
    for i = 1:n_bids
        AREA = bidList(i,3);
        bids(AREA) = bids(AREA) + 1;
    end
    M = max(bids);
    % Set size of bid matrices
    Q_min = zeros(N,M); Q_max = zeros(N,M); C = zeros(N,M);
    % Set data from bidList to bid matrices
    counter = zeros(1,N);
    for i = 1:n_bids
      PRICE = bidList(i,1); QUANTITY = bidList(i,2); AREA = bidList(i,3);
      if AREA <= N
            counter(AREA) = counter(AREA) + 1;
            C(AREA, counter(AREA)) = PRICE;
            if QUANTITY < 0
                Q_min(AREA, counter(AREA)) = QUANTITY;
                Q_max(AREA, counter(AREA)) = 0;
            else
                Q_min(AREA, counter(AREA)) = 0;
                Q_max(AREA, counter(AREA)) = QUANTITY;
            end
      end
    end
    if bids ~= counter
        msg = 'Error: generateBidMat - Matrix counter mismatch \n';
        error(msg)
    end
end
```

Listing 7.1: Matlab function for generating bid matrices

```
%% Init file for Simulink model power_system_v2.11.slx
clear all;

%% SYSTEM WIDE SETTINGS
N = 11; % Number of control areas
L = 2500; % [MW] Area power base value
sim_time = 1000;

% CONTROL CENTER
% Sample time for generating new AGC set-points
sample_time_frr_a = 10;

% Extract FRR-A bids to matrices
bidListUp = xlsread('FRR-A_bids_all_up.xlsx');
bidListDown = xlsread('FRR-A_bids_all_down.xlsx');
[Q_min_up, Q_max_up, C_up] = generateBidMat(bidListUp, N);

% Optimization paramters
flowCost = 0.001;
activationCost = 1;

% Model of admittance used to predict flow
Y_m = 3.00;
Ymat_pred = ...
[0   Y_m  Y_m 0   Y_m 0   0   Y_m 0   0   0;
Y_m  0    0   0   Y_m 0   0   0   0   0   0;
Y_m  0    0   Y_m Y_m 0   Y_m 0   0   0   0;
0    0    Y_m 0   0   Y_m Y_m 0   0   Y_m 0;
Y_m  Y_m  Y_m 0   0   0   0   0   0   0   0;
0    0    0   Y_m 0   0   Y_m 0   0   Y_m 0;
0    0    Y_m Y_m 0   Y_m 0   Y_m 0   0   0;
Y_m  0    0   0   0   0   Y_m 0   Y_m 0   0;
0    0    0   0   0   0   0   Y_m 0   0   Y_m;
0    0    0   Y_m 0   Y_m 0   0   0   0   0;
0    0    0   0   0   0   0   0   Y_m 0   0];

% Generate B_prime matrix
B_prime = (diag(sum(Ymat_pred,2)') - Ymat_pred);

% Negative suseptence
D = diag(Y_m);

% Tie-line connection matrix
% [branches, nodes]
A = [1   -1  0   0   0   0   0   0   0   0   0;   % B1
     1   0   -1  0   0   0   0   0   0   0   0;   % B2
     1   0   0   0   -1  0   0   0   0   0   0;   % B3
     1   0   0   0   0   0   0   -1  0   0   0;   % B4
     0   1   0   0   -1  0   0   0   0   0   0;   % B5
     0   0   1   0   -1  0   0   0   0   0   0;   % B6
     0   0   1   -1  0   0   0   0   0   0   0;   % B7
     0   0   1   0   0   0   -1  0   0   0   0;   % B8
     0   0   0   1   0   -1  0   0   0   0   0;   % B9
     0   0   0   1   0   0   -1  0   0   0   0;   % B10
     0   0   0   1   0   0   0   0   0   -1  0;   % B11
     0   0   0   0   0   1   -1  0   0   0   0;   % B12
     0   0   0   0   0   1   0   0   0   -1  0;   % B13
```

```
      0   0   0   0   0   0   1   -1   0   0   0;   % B14
      0   0   0   0   0   0   0   1   -1   0   0;   % B15
      0   0   0   0   0   0   0   0   1   0   -1]; % B16

% Capacity
minFlowVector = [-100 -100 -100 -100 -100 -100 -100 -100 ...
                 -100 -100 -100 -100 -100 -1000 -100 -100];
maxFlowVector = [100 100 100 100 100 100 100 100 ...
                 100 100 100 100 100 100 100 100];

%% POWER SYSTEM MODEL
% Parameters for control areas
% parameters = [Tg2 T_w H EMPTY 1/R beta EMPTY Ti]
param_NO1 = [5 1.5 3.5 0 0.25 0.26 0 200];
param_NO2 = [5 1.5 3.5 0 0.24 0.26 0 200];
param_NO3 = [5 1.5 3.5 0 0.25 0.25 0 200];
param_NO4 = [5 1.5 3.5 0 0.35 0.34 0 200];
param_NO5 = [5 1.5 3.5 0 0.30 0.26 0 200];
param_SE1 = [5 1.5 3.5 0 0.26 0.27 0 200];
param_SE2 = [5 1.5 3.5 0 0.25 0.26 0 200];
param_SE3 = [5 1.5 3.5 0 0.23 0.24 0 200];
param_SE4 = [5 1.5 3.5 0 0.22 0.23 0 200];
param_FI =  [5 1.5 3.5 0 0.22 0.25 0 200];
param_DK2 = [5 1.5 3.5 0 0.18 0.19 0 200];

% Tie-line connection matrix #2
branches = [1 2; 1 3; 1 5; 1 8; 2 5; 3 5; 3 4; 3 7; ...
            4 6; 4 7; 4 10; 6 7; 6 10; 7 8; 8 9; 9 11];
% Tie-line admittances used to model flow
Y = [3.00 3.10 2.90 3.15 2.98 ...
     2.95 3.16 2.97 3.01 2.87 3.22 3.14 2.89 2.95 2.85 3.01];
% Admittance matrix
Ymat = ...
[0     Y(1)  Y(2)  0     Y(3)  0     0     Y(4)  0     0     0;
Y(1)  0     0     0     Y(5)  0     0     0     0     0     0;
Y(2)  0     0     Y(7)  Y(6)  0     Y(8)  0     0     0     0;
0     0     Y(7)  0     0     Y(9)  Y(10) 0     0     Y(11) 0;
Y(3)  Y(5)  Y(6)  0     0     0     0     0     0     0     0;
0     0     0     Y(9)  0     0     Y(12) 0     0     Y(13) 0;
0     0     Y(8)  Y(10) 0     Y(12) 0     Y(14) 0     0     0;
Y(4)  0     0     0     0     0     Y(14) 0     Y(15) 0     0;
0     0     0     0     0     0     0     Y(15) 0     0     Y(16);
0     0     0     Y(11) 0     Y(13) 0     0     0     0     0;
0     0     0     0     0     0     0     0     Y(16) 0     0];

% Tie-line damping
D_tieline = 0.05;
```

Listing 7.2: Init file for Simulink model

```
%% Optimal FRR-A Allocation Function
% Requres YALMIP and solvers
function [production, export, flow_d, shortage, bids, FRR_A_cost] ...
        = optimalFRRAallocation(demands, Q_min, Q_max, C, B_prime, D, A
    ,...
          minFlowVector, maxFlowVector, flowCost, activationCost)
fprintf('\n\n********** ALLOCATING PRODUCTION... **********\n');
demand = sum(demands);
[n, m] = size(Q_max);
if demand < 0
    fprintf('Production DOWN\n');
    if sum(sum(Q_min)) > demand
        fprintf('NOT ENOUGH BIDS TO COVER DEMAND\n');
    end
else
    fprintf('Production UP\n');
    if sum(sum(Q_max)) < demand
        fprintf('NOT ENOUGH BIDS TO COVER DEMAND\n');
    end
end
fprintf('***** Finding solution... ***** \n');

% Decision variables
onoff = binvar(n,m,'full');
P = sdpvar(n,m,'full');
prod_slack = sdpvar(n,1,'full');
delta = sdpvar(n,1,'full');
delta(1) = 0; % Phase angle reference

% Help variables
flow = D*A*delta;
prod = sum(P,2);

% Set contraints
matchTotalDemand = sum(prod) == demand;
noOverproduction = prod_slack >= 0;
bidSizeMin = onoff .* Q_min <= P;
bidSizeMax = P <= onoff .* Q_max;
findAngles = prod - demands == B_prime*delta;
findAnglesWithSlack = prod - demands + prod_slack == B_prime*delta;
flowCapMin = flow >= minFlowVector;
flowCapMax = flow <= maxFlowVector;

Constraints = [matchTotalDemand bidSizeMin bidSizeMax findAngles ...
                flowCapMin flowCapMax];

% Set objective function
powerCost = sum(sum(C .* abs(P)));
clogCost = flowCost*sum(abs(flow));
prodSlackCost = sum(prod_slack)*10000;
actCost = activationCost * sum(sum(onoff));

Objective = powerCost + clogCost + actCost;

% Solve the problem
res = optimize(Constraints,Objective)
no_solution = res.problem;
```

```
57
58 % If no feasible solution, get best effort solution
59 if no_solution
60   fprintf('\n ***** No feasible solution. Demand cannot be met. ***** \n')
       ;
61   fprintf('***** Finding best-effort solution... ***** \n');
62   Constraints = [noOverproduction bidSizeMin bidSizeMax ...
63                  findAnglesWithSlack flowCapMin flowCapMax];
64   Objective = powerCost + clogCost + activationCost + prodSlackCost;
65   res = optimize(Constraints,Objective)
66   no_solution = res.problem;
67   if no_solution
68     fprintf('ERROR: No solution. Applying zero FRR-A production \n');
69   else
70     fprintf('***** Best-effort solution found ***** \n');
71   end
72 else
73     fprintf('***** Solution found ***** \n');
74     prod_slack = zeros(n,1);
75 end
76
77 % Store result in variables, set numbers smaller than 'eps' to zero
78 eps = 1e-8;
79 bids = value(P); bids(abs(bids)<eps)=0;
80 production = value(prod); production(abs(production)<eps)=0;
81 shortage = value(prod_slack); shortage(abs(shortage)<eps)=0;
82 cost.power = value(powerCost);
83 cost.clog = value(clogCost);
84 cost.activation = value(activationCost);
85 FRR_A_cost = cost.power;
86 export = production - demands;
87 flow_d = value(flow);
88
89 %  If no solution, apply zero FRR-A production
90 if no_solution
91     bids = zeros(n,m);
92     production = zeros(n,1);
93     shortage = demands;
94     cost.power = 0;
95     cost.clog = 0;
96     cost.activation = 0;
97     FRR_A_cost = cost.power;
98     export = production - demands;
99 end
100
101 % Print to Matlab
102 prod_array = production';
103 flow_array = flow_d';
104 shortage_array = shortage';
105 prod_array
106 flow_array
107 shortage_array
108 cost
109 fprintf('********** DONE ***************\n');
```

Listing 7.3: Matlab function for solving MILP problem

B Simulink Diagrams

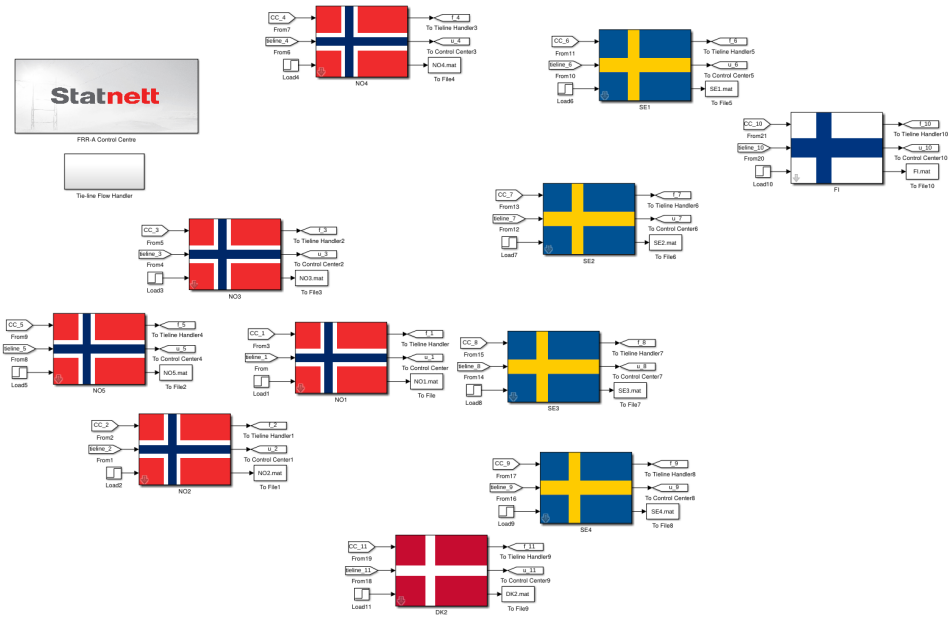

Figure 7.1: Simulink diagram of Nordic power system

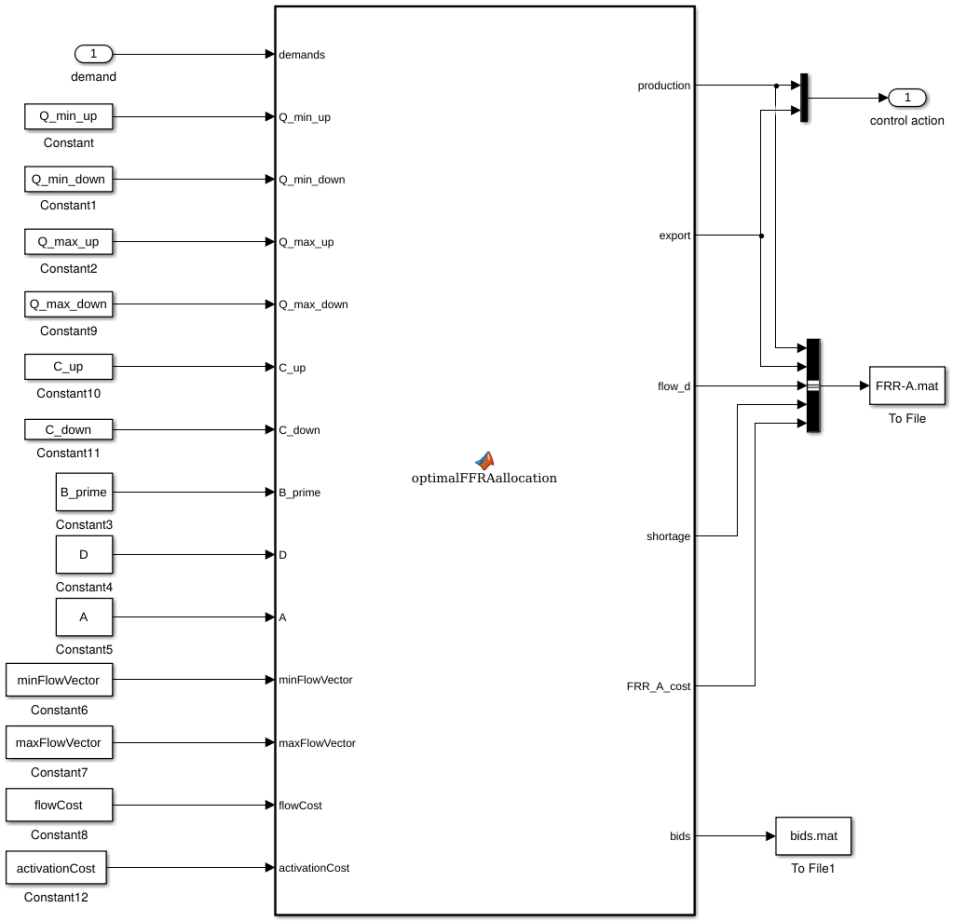

Figure 7.2: Simulink diagram of optimal FRR-A allocation

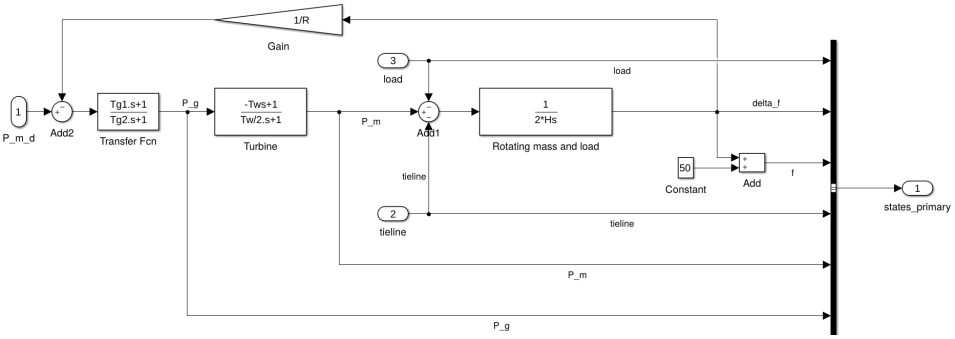

Figure 7.3: Simulink diagram of generating unit with primary control

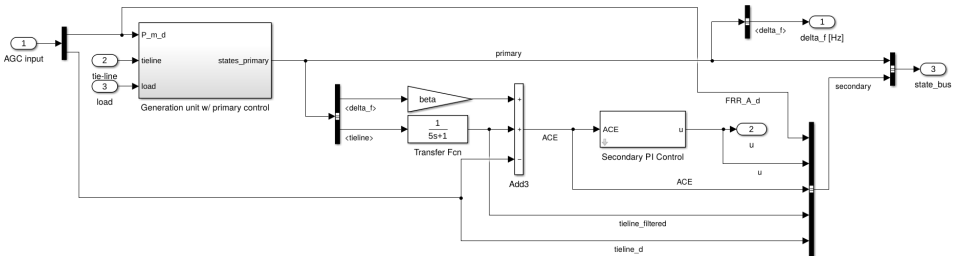

Figure 7.4: Simulink diagram of secondary control loop

C FRR-A Bid Lists

UP REGULATION					DOWN REGULATION				
Price	Quantity	Area	Power Plant	Type	Price	Quantity	Area	Power Plant	Type
[NOK/MW]	[MW]				[NOK/MW]	[MW]			
33.09	112	4	Siso	Hydro	-98.45	-14	11	DONGTP-E	Thermal
33.09	11	5	Fortun	Hydro	-35	-30	10		Hydro
33.68	24	5	Tyin	Hydro	-33	-30	10		Hydro
33.95	12	7	Faxälven Nedre	Hydro	-32.2	-10	7	Nedre ume älv	Hydro
34.2	10	7	Nedre ume älv	Hydro	-31.69	-12	7	Faxälven Nedre	Hydro
34.27	20	2	SKL	Hydro	-31	-50	10		Hydro
34.27	13	2	Tjodan	Hydro	-30.56	-10	6	Skellefteälven N	Hydro
34.27	10	2	Tokke	Hydro	-30	-50	10		Hydro
35.45	50	5	BKK	Hydro	-29.7	-46	8	Norsälven	Hydro
35.45	25	5	Fortun	Hydro	-29.54	-25	3	Åskåra	Hydro
35.45	18	2	Hjartdøla	Hydro	-29.2	-10	7	Järpen	Hydro
36.04	70	5	Aurland	Hydro	-29.2	-10	7	Järpen	Hydro
36.04	20	2	SKL	Hydro	-29	-10	10		Thermal
36.04	16	1	Hedmark	Hydro	-29	-12	10		Hydro
36.22	10	6	Skellefteälven N	Hydro	-29	-50	10		Hydro
36.63	48	2	Ulla-Førre	Hydro	-29	-205	6	Ritsem	Hydro
36.63	11	4	Sulitjelma	Hydro	-28.8	-15	8	Byälven	Hydro
36.63	10	5	Uvdal	Hydro	-28.8	-20	7	Järpen	Hydro
37.22	21	5	Sima	Hydro	-28.8	-32	8	Norsälven	Hydro
37.35	20	7	Åseleälv	Hydro	-28.36	-10	5	Naddvik	Hydro
37.7	28	6	Ritsem	Hydro	-28.36	-12	2	Tokke	Hydro
37.8	35	6	Harspränget	Hydro	-28.36	-15	4	Siso	Hydro
37.81	25	5	Fortun	Hydro	-28.29	-61	7	Sällsjö	Hydro
38	65	8	Trängslet BKB	Hydro	-28.29	-100	7	Ljungan Övre	Hydro
38	38	6	Ritsem	Hydro	-28	-29	7	Järpen	Hydro
38.4	18	5	Sima	Hydro	-27.9	-14	8	Norsälven	Hydro
38.5	17	6	Ritsem	Hydro	-27.9	-15	7	Järpen	Hydro
38.99	35	5	Jostedal	Hydro	-27.9	-38	7	Järpen	Hydro
38.99	14	2	Ulla-Førre	Hydro	-27.9	-105	8	Trängslet BKB	Hydro
38.99	10	2	Saudefaldene	Hydro	-27.77	-14	5	SFE	Hydro
39.3	15	6	Ritsem	Hydro	-27.77	-24	2	Saudefaldene	Hydro
39.59	20	5	BKK	Hydro	-27.77	-48	5	Svelgen	Hydro
40	35	6	Harspränget	Hydro	-27.77	-102	3	Åskåra	Hydro
40.18	103	5	Aurland	Hydro	-27.77	-133	3	Grytten	Hydro
40.18	25	5	Fortun	Hydro	-27.18	-10	5	Leirdøla	Hydro
40.74	55	7	Indalsälven Övr	Hydro	-27.18	-20	5	Borgund	Hydro
40.77	15	2	Tokke	Hydro	-27.18	-32	4	Skjomen	Hydro
41.88	5	9	GrundRO SN4	Hydro	-27.18	-34	4	Sulitjelma	Hydro
42.54	120	5	Aurland	Hydro	-27.18	-50	5	Tyin	Hydro
42.54	13	4	Siso	Hydro	-27	-15	8	Gullspång	Hydro
42.54	10	2	Tokke	Hydro	-27	-15	10		Thermal
42.54	10	5	Sima	Hydro	-27	-40	6	Harspränget	Hydro
42.6	113	6	Harspränget	Hydro	-27	-50	10		Hydro
43	10	8	StoraEnso/Kvar	Consumption	-26.59	-10	2	Saudefaldene	Hydro
43.72	10	5	Borgund	Hydro	-26.59	-20	2	SKL	Hydro
44.31	250	5	Sima	Hydro	-26.59	-33	5	Jostedal	Hydro
44.31	15	2	Ulla-Førre	Hydro	-26.59	-50	5	Tyin	Hydro
44.4	30	8	Trängslet BKB	Hydro	-26.2	-10	7	Järpen	Hydro
44.9	23	2	Holen	Hydro	-26.1	-20	7	Järpen	Hydro
45.49	154	2	Ulla-Førre	Hydro	-26.03	-40	7	Åseleälv	Hydro
45.49	25	5	Naddvik	Hydro	-26.03	-51	6	Rebnis	Hydro
46.08	10	3	Driva	Hydro	-26	-27	2	Tokke	Hydro
46.6	25	6	Messaure	Hydro	-26	-40	4	Siso	Hydro
47.27	25	3	Tafjord	Hydro	-26	-45	2	Rjukanverkene	Hydro
47.27	10	2	SKL	Hydro	-26	-50	5	Tyin	Hydro
47.86	124	5	Leirdøla	Hydro	-26	-53	2	Tokke	Hydro
47.86	118	3	Aura	Hydro	-26	-60	2	Ulla-Førre	Hydro
49.04	297	4	Kobbelv	Hydro	-26	-62	1	Dokka	Hydro
50.5	31	6	Messaure	Hydro	-26	-68	2	Tjodan	Hydro
51.4	15	8	Trängslet BKB	Hydro	-26	-91	5	Aurland	Hydro

UP REGULATION					DOWN REGULATION				
Price	Quantity	Area	Power Plant	Type	Price	Quantity	Area	Power Plant	Type
[NOK/MW]	[MW]				[NOK/MW]	[MW]			
52.58	250	4	Rana	Hydro	-26	-190	5	Sima	Hydro
53.17	30	3	Tafjord	Hydro	-26	-230	5	Folgefonn	Hydro
54.36	16	5	Vik	Hydro	-26	-260	5	Sima	Hydro
54.36	10	3	KVO	Hydro	-25.46	-10	6	Kvistforsen	Hydro
54.88	10	10		Consumption	-25.41	-14	2	Tokke	Hydro
54.95	51	4	Skjomen	Hydro	-25.41	-42	2	Ulla-Førre	Hydro
54.95	23	4	Innset/Straums	Hydro	-25.41	-50	5	BKK	Hydro
56.72	15	4	Røssåga	Hydro	-25.41	-50	5	Tyin	Hydro
59	10	10		Thermal	-25.41	-141	5	Aurland	Hydro
59.08	20	5	BKK	Hydro	-25.41	-260	5	Sima	Hydro
60	10	10		Thermal	-25.2	-33	7	Järpen	Hydro
60.3	16	11	EDK-E	Thermal	-25	-10	10		Hydro
61	10	10		Hydro	-25	-10	10		Thermal
62.31	11	11	DANCOM-E	Thermal	-25	-30	10		Thermal
63.22	41	3	Nea	Hydro	-25	-120	7	Övre Ångerm.äl	Hydro
63.81	21	5	Høyanger	Hydro	-24.9	-38	7	Fjällsjö Övre	Hydro
64.99	10	3	KVO	Hydro	-24.9	-44	7	Blåsjön	Hydro
67.35	42	3	Nea	Hydro	-24.81	-30	5	Hallingdal	Hydro
69	30	10		Hydro	-24.81	-35	5	Uvdal	Hydro
70	20	10		Thermal	-24.81	-35	5	Naddvik	Hydro
70.9	25	3	NTE	Hydro	-24.81	-36	5	Leirdøla	Hydro
70.9	24	4	Adamselv	Hydro	-24.81	-40	5	Svelgen	Hydro
70.9	10	2	Sira-Kvina	Hydro	-24.81	-50	5	Tyin	Hydro
71.03	10	11	NEEY-E	Thermal	-24.81	-87	4	Skjomen	Hydro
71.49	37	5	Vik	Hydro	-24.8	-10	7	Ljusnan Mell. S	Hydro
73.85	57	3	Nea	Hydro	-24.33	-45	7	Indalsälven Övr	Hydro
75.03	23	4	Adamselv	Hydro	-24.22	-33	5	Bjølvo	Hydro
76.12	11	11	NEEY-E	Thermal	-24.22	-40	5	Tyin	Hydro
76.81	20	3	KVO	Hydro	-24.22	-41	2	HER	Hydro
77.4	20	3	Aura	Hydro	-24.22	-64	2	Flørli	Hydro
78	30	10		Hydro	-24.22	-135	2	Ulla-Førre	Hydro
78.58	35	5	Høyanger	Hydro	-24.22	-197	5	Jostedal	Hydro
80	10	10		Thermal	-24	-10	7	Järpen	Hydro
80.41	19	11	EDK-E	Thermal	-24	-15	10		Thermal
83.76	11	11	NEEY-E	Thermal	-24	-34	8	Klarälven	Hydro
85	30	10		Thermal	-23.77	-30	7	Ume Nedre SK	Hydro
88.62	80	2	Sira-Kvina	Hydro	-23.63	-20	2	SKL	Hydro
88.62	10	3	TEK	Hydro	-23.63	-21	1	Valdres	Hydro
89.52	10	11	NEEY-E	Thermal	-23.63	-22	2	Sundsbarm	Hydro
90	10	10		Hydro	-23.63	-30	4	Sundsfjord	Hydro
92.17	98	5	Nore	Hydro	-23.63	-35	2	HER	Hydro
94.9	18	6	Letsi	Hydro	-23.63	-44	4	Svartisen	Hydro
95.9	127	6	Letsi	Hydro	-23.63	-50	5	BKK	Hydro
97	10	10		Consumption	-23.63	-50	5	Hallingdal	Hydro
100	10	10		Consumption	-23.63	-54	4	Kolsvik	Hydro
100	10	10		Hydro	-23.63	-60	3	Tafjord	Hydro
107.21	17	11	EDK-E	Thermal	-23.63	-87	2	Tokke	Hydro
112.26	50	3	Tafjord	Hydro	-23.63	-89	2	Ulla-Førre	Hydro
118.16	70	2	Sira-Kvina	Hydro	-23.63	-90	2	Sira-Kvina	Hydro
125	10	10		Hydro	-23.3	-30	7	Järpen	Hydro
134.01	12	11	NEEY-E	Thermal	-23.2	-10	6	Kvistforsen	Hydro
135	10	10		Hydro	-23.2	-35	7	Fjällsjö Övre	Hydro
140	14	10		Consumption	-23.04	-19	2	Mår	Hydro
141.8	10	2	SKL	Hydro	-23.04	-30	2	Rjukanverkene	Hydro
150	20	10		Consumption	-23.04	-36	2	Tokke	Hydro
150	10	10		Hydro	-23.04	-99	4	Rana	Hydro
150	10	10		Hydro	-23	-10	8	StoraEnso/Kvar	Consumption
153.61	10	5	BKK	Hydro	-23	-10	10		Hydro
169.77	15	8	E-SANDVIK	Consumption	-23	-10	10		Hydro
170	10	8	Snitt 3 avkoppl.l	Consumption	-23	-10	10		Hydro

Figure 7.5: Bids used in the optimal FRR-A allocation (Only first 120 bids included)